JCI insight

Endothelial HIFα-PDGF-B to smooth muscle Beclin1 signaling sustains pathological muscularization in pulmonary hypertension

Fatima Z. Saddouk, … , Junichi Saito, Daniel M. Greif

JCI Insight. 2024. https://doi.org/10.1172/jci.insight.162449.

Research In-Press Preview Pulmonology Vascular biology

Graphical abstract

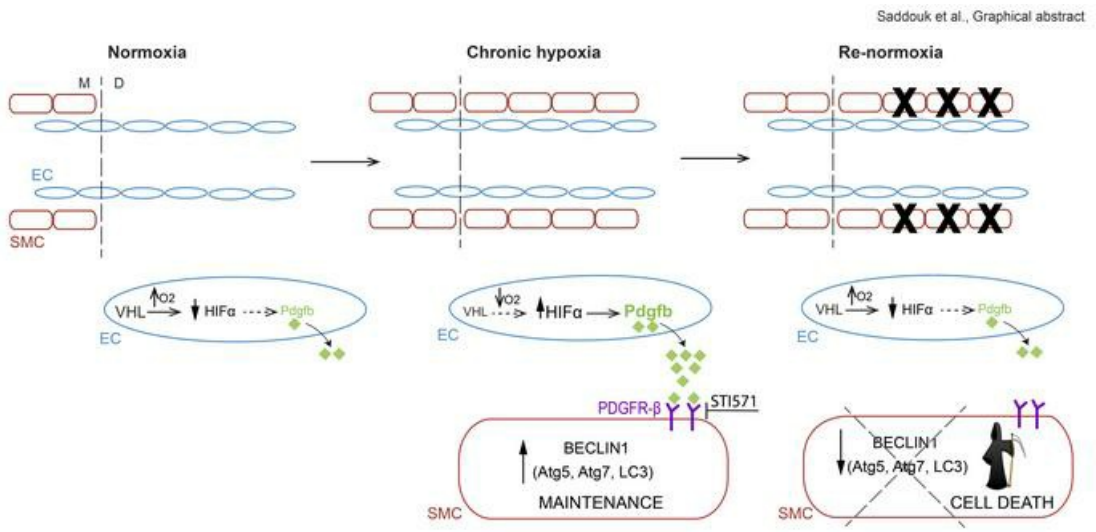

Find the latest version:

https://jci.me/162449/pdf

Endothelial HIFα-PDGF-B to smooth muscle Beclin1 signaling sustains pathological muscularization in pulmonary hypertension

Fatima Z. Saddouk[1,2], Andrew Kuzemczak[1,2], Junichi Saito[1,2], Daniel M. Greif[1,2,*]

[1]Yale Cardiovascular Research Center, Section of Cardiovascular Medicine,
Department of Internal Medicine, [2]Department of Genetics,
Yale University, New Haven, CT 06511, USA

*To whom correspondence should be addressed: Daniel M. Greif, 300 George St., Yale Cardiovascular Research Center, Yale University, New Haven, CT 06511, USA.
daniel.greif@yale.edu (email), 203-737-2040 (phone), 203-737-6118 (FAX)

The authors have declared that no conflict of interest exists.

Conflict of interest: The authors have declared that no conflicts of interest exist.

Abstract

Mechanisms underlying maintenance of pathological vascular hypermuscularization are poorly delineated. Herein, we investigated retention of smooth muscle cells (SMCs) coating normally unmuscularized distal pulmonary arterioles in pulmonary hypertension (PH) mediated by chronic hypoxia +/- Sugen 5416, and reversal of this pathology. With hypoxia in mice or culture, lung endothelial cells (ECs) upregulated hypoxia-inducible factor (Hif)-1a and 2a which induce platelet-derived growth factor-B (PDGF-B), and these factors reduced to normoxic levels with re-normoxia. Re-normoxia reversed hypoxia-induced pulmonary vascular remodeling, but with EC HIFα over-expression during re-normoxia, pathological changes persisted. Conversely, after establishment of distal muscularization and PH, EC-specific deletion of *Hif1a*, *Hif2a* or *Pdgfb* induced reversal. In human idiopathic pulmonary artery hypertension, HIF1A, HIF2A, PDGFB and autophagy-mediating gene products, including Beclin1, were upregulated in pulmonary artery SMCs and/or lung lysates. Furthermore, in mice, hypoxia-induced EC-derived PDGF-B upregulated Beclin1 in distal arteriole SMCs, and after distal muscularization was established, re-normoxia, EC *Pdgfb* deletion or treatment with STI571 (which inhibits PDGF receptors) downregulated SMC Beclin1 and other autophagy products. Finally, SMC-specific *Becn1* deletion induced apoptosis, reversing distal muscularization and PH mediated by hypoxia +/- Sugen 5416. Thus, chronic hypoxia induction of HIFα-to-PDGF-B axis in ECs is required for non-cell autonomous Beclin1-mediated survival of pathological distal arteriole SMCs.

Introduction

Chronic cardiovascular diseases, such as atherosclerosis, arterial restenosis and pulmonary hypertension (PH), are characterized by excess and aberrant smooth muscle cells (SMCs). The processes leading to this hypermuscularization are highly studied whereas once pathological SMCs are established, mechanisms - both cell autonomous and non-cell autonomous - responsible for their maintenance are not well understood. In pulmonary artery hypertension (PAH; classified by the World Health Organization as Group 1 PH), reduced compliance of the pulmonary vasculature predicts mortality (1), and the distal extension of SMCs to normally unmuscularized pulmonary arterioles reduces compliance. PAH treatments primarily induce vascular dilation but generally do not ameliorate hypermuscularization, and unfortunately, this disease remains highly morbid and lethal with ~50% of patients dying within seven years of diagnosis (2). From a therapeutic standpoint, it is critical to elucidate how to reverse distal arteriole muscularization because when symptomatic patients initially present for clinical evaluation invariably their distal pulmonary arterioles are muscularized. Thus, a fundamental question arises: what cellular processes and molecular pathways can be manipulated to reverse pathological remodeling?

High altitude residents and acclimatized climbers are at risk for developing muscularized distal pulmonary arterioles and PH due to hypobaric hypoxia, and relocation to lower altitudes often normalizes pulmonary artery pressure (3-6). This exposure to increased oxygen levels at lower altitudes is thought to also result in regression of distal arteriole muscularization (5, 6). In rats, re-exposure to normoxia following hypoxia induces vascular cell apoptosis and reverses pathological vascular remodeling (7, 8). Apoptosis resistance of pulmonary artery (PA) SMCs is a hallmark of PH, and during re-oxygenation, there is an increase in apoptosis that contributes to

the regression of vascular remodeling (8). However, the cellular events underlying reversal and the molecular mechanisms regulating this process are poorly understood.

Hypoxia-inducible factors (HIFs) modulate gene transcription in an oxygen-dependent manner and are key players in inducing pulmonary vascular remodeling and PH (9-11). HIFs are heterodimers of HIF1-β and either HIF1-α or HIF2-α. Mice heterozygous for the global null allele *Hif1a* or *Hif2a* or with SMC-specific deletion of *Hif1a* via *Myh11-CreER*^{T2}, *Hif1a*$^{(flox/flox)}$ have attenuated hypoxia-induced PH and lung vascular disease (12-14). Similarly, *Hif2a*$^{(flox/flox)}$ mice with *Hif2a* deletion conditionally in ECs with *Tie2-CreER*^{T2} or constitutively in pulmonary ECs with *L1-Cre* are protected against PH (15, 16). However, in established disease, the roles of HIFs in retention of pathological SMC remodeling under chronic hypoxia and its reversal are not well studied.

Hypoxia induces EC expression of diverse growth factors and agonists that non-cell autonomously regulate the biology of PASMCs and are implicated in PH and pulmonary vascular remodeling (17-20). We have previously shown that a hypoxia-induced EC HIF1-α to platelet derived growth factor (PDGF)-B pathway regulates PASMC proliferation and de-differentiation (10). Yet, whether ECs play a key role in sustaining distal arteriole muscularization and its reversal has not been investigated. PDGF-B induces autophagy in SMCs (21, 22). Beclin1 is a critical initiator of the autophagic pathway, and Beclin1 expression is upregulated in hypoxia-induced PH and is positively related to autophagy in PH (23, 24). Enhanced migration and proliferation of *Becn1*$^{(+/-)}$ lung ECs is dependent on HIF2-α (25). However, the pathophysiological functions of Beclin1 in PH and vascular remodeling are not well studied.

In the current study, we demonstrate that ECs are non-cell autonomously essential for the retention of established hypoxia-induced distal arteriole SMCs. SMC HIFα is not required for sustaining pathological distal arteriole muscularization, whereas deletion of *Hif1a* or *Hif2a* in ECs following hypoxia-induced distal arteriole muscularization leads to reversal of this muscularization despite continued hypoxia. HIF1-α and HIF2-α regulate Pdgfb expression under chronic hypoxia, and *Pdgfb* deletion in ECs following hypoxia-induced distal arteriole muscularization reverses this pathology highlighting the importance of EC-SMC interactions in the retention of pathological hypermuscularization. Finally, we show the non-cell autonomous effects of EC-derived PDGF-B induction of PASMC Beclin1 and that the latter is essential for the retention of distal arteriole muscularization by augmenting autophagy and inhibiting apoptosis of SMCs.

Results

Re-normoxia reverses hypoxia-induced distal arteriole muscularization and PH

The distal extension of smooth muscle coverage to normally unmuscularized distal pulmonary arterioles is a hallmark of human and rodent PH (26-28). As in our prior studies, we focus on specific pulmonary arteriole beds adjacent to identified airway branches (left bronchus-first lateral secondary branch-first anterior branch or left bronchus-first medial branch) in the adult mouse lung (10, 27-29) (Fig. S1A). Muscularized pulmonary arteries and arterioles are identified by their continuous layer of α-smooth muscle actin $(SMA)^+$ SMCs whereas pulmonary veins have a coating of SMCs that form a relatively loose mesh around the vessel (30), and *Bmx-CreER*^{T2} marks ECs of arteries and arterioles but not venous ECs (Fig. S1B) (31). Distal arterioles in these beds are unmuscularized normally but with hypoxia exposure undergo a

stereotyped process of muscularization, resulting in PH and right ventricle hypertrophy (RVH) (27, 28). Herein, we investigate these specific arteriole beds to assess the reversal of hypoxia-induced vascular remodeling upon re-normoxia.

To evaluate whether hypoxia-induced distal arteriole muscularization, RVH and/or PH in mice are reversible, *Bmx-CreER*^{T2}*, ROSA26R*$^{(mTmG/mTmG)}$ or wild type mice were exposed to hypoxia (FiO_2 10%) for 21 days and then transferred to re-normoxia (FiO_2 21%) for up to 28 or 42 days, respectively (Figs. 1A, S1C). Distal muscularization starts to regress by re-normoxia day 14 (Figs. 1B, C, S1D) and by day 21 there is a significant reduction in the right ventricle systolic pressure (RVSP; equivalent to pulmonary artery systolic pressure) and weight ratio of right ventricle (RV) to the sum of the left ventricle (LV) and septum (S), which is a measure of RVH (Fig. 1D, E). By re-normoxia day 42, the three parameters measured - distal muscularization, RVSP and RV weight ratio - are normalized and do not differ significantly from the basal normoxic state. We then investigated whether hypoxia-induced distal muscularization can be recapitulated by exposing these recovered mice to hypoxia once again. Mice were exposed to 21 days of hypoxia followed by normoxia for 42 days and then re-exposed to hypoxia for 21 days (Fig. 1F). Mice re-exposed to hypoxia develop distal arteriole muscularization, PH and RVH, at levels equivalent to the initial 21 day hypoxic mice (Fig. 1G-J).

Given that re-normoxia leads to reversal of hypoxia-induced distal muscularization in mice, we next evaluated whether distal arteriole SMCs downregulate SMA expression and change fate or undergo cell death during the re-normoxia phase. *Acta2-CreER*^{T2}*, ROSA26R*$^{(mTmG/+)}$ mice were induced with tamoxifen, rested for 5 days and then either exposed to: i) normoxia for an additional 32 days; ii) hypoxia for 21 days or iii) hypoxia for 21 days, followed by re-normoxia for 42 days (Fig. S2A). In agreement with our prior results (27), at

hypoxia day 21, the vast majority of distal arteriole SMCs are GFP^+ indicating that they derive from pre-existing SMCs (Fig. S2B). With re-normoxia, only very rare distal arteriole SMA^+ cells persist and these cells are invariably GFP^+, and essentially all GFP^+ lung cells are SMA^+ (Fig. S2B). Thus, distal arteriole SMCs do not undergo a fate change (e.g., de-differentiation or trans-differentiation) to a SMA^- cell type with re-normoxia. Furthermore, at day 7 of re-normoxia, 7±1% of distal arteriole SMCs are $TUNEL^+$ (Fig. S2C, D), indicating that similar to prior studies in rats (8), exposure to re-normoxia induces programmed cell death of SMCs coating small vessels.

SMC HIFα is neither necessary nor sufficient for retention of distal arteriole muscularization

Hypoxia-inducible factors (HIFs) are heterodimers of HIF1-β and either HIF1-α or HIF2-α. Herein, mRNA and protein levels of Hif1a, Hif2a and their transcriptional target Bnip3 (BCL2 Interacting Protein 3) were found to be upregulated in whole lung lysates of mice exposed to hypoxia for 21 days and then decreased when mice are returned to normoxia for 7 or 14 days (Fig. 2A-C). In PASMCs, HIF1-α is the main isoform as HIF2-α is not readily detectable (32), and *Hif1a* deletion in SMCs protects mice against hypoxia-induced distal pulmonary arteriole muscularization and PH (10, 14). To investigate dynamics of SMC Hif1a levels in the context of PH reversal, Zs^+ cells were isolated by fluorescence activated cell sorting (FACS) from the lungs of tamoxifen-induced *Acta2-CreER*^{T2}, *ROSA26R*$^{(Zs/+)}$ mice exposed to normoxia, hypoxia or hypoxia followed by 10 days of re-normoxia. The marked hypoxia-induced Hif1a levels in Zs^+ SMCs is mitigated upon re-normoxia (Fig. 2D). Because HIFα in ECs is critical for developing distal pulmonary arteriole muscularization and PH in response to hypoxia (10, 15, 33), we next

evaluated the role of EC HIFα in sustaining these pathological changes with chronic hypoxia. Lung ECs were isolated by FACS from mice exposed to either normoxia, hypoxia or hypoxia followed by 10 days of re-normoxia, and HIF1-α and HIF2-α levels increase with hypoxia and then decrease with re-normoxia (Fig. 2E-G).

Based on the dynamics of HIFα expression and distal pulmonary arteriole muscularization, we initially postulated that SMC HIF-1α may play a key role in sustaining distal muscularization and PH under hypoxic conditions. To investigate this hypothesis, *Acta2-CreER*^{T2}*, Hif1a*$^{(flox/flox)}$ mice were exposed to hypoxia for 49 days and tamoxifen (1 mg/day) was or was not administered on days 17-21 to delete *Hif1a* (Fig. S3A). Surprisingly, tamoxifen-induced *Hif1a* deletion in SMCs has no effect on distal muscularization, PH or RVH in hypoxic mice (Fig. S3B-D). We next employed a complementary strategy to upregulate HIFα in SMCs under normoxic conditions. HIFα is kept at a low level in normoxia by proline hydroxylation which facilitates binding to the von-Hippel Lindau (VHL)-E3 ubiquitin ligase complex, resulting in protein ubiquitination and degradation (34, 35). In contrast, HIFα accumulates with hypoxia because oxygen is not available as a substrate for proline hydroxylation. Under normoxic conditions, *Acta2-CreER*^{T2} or *Acta2-CreER*^{T2}*, ROSA26R*$^{(Zs/+)}$ mice also carrying *Vhl*$^{(flox/flox)}$ or wild type for *Vhl* were induced with tamoxifen and analyzed 5 days later to assess deletion efficiency (Fig. S4A). Lung Zs^{+} SMCs were isolated by FACS, and qRT-PCR shows a ~70% deletion efficiency of Vhl and 3-fold upregulation of Hif1a (Fig. S4B). Similarly, at the protein level, tamoxifen treatment of *Acta2-CreER*^{T2}*, Vhl*$^{(flox/flox)}$ mice markedly reduced VHL in SMCs and upregulated HIF1-α in lung lysates (Fig. S4C-E). Next, *Acta2-CreER*^{T2}*, Vhl*$^{(flox/flox)}$ mice were treated with tamoxifen and rested for 37 days in normoxia, which does not induce distal muscularization, PH or RVH (Fig. S4F-I). In a subsequent set of experiments, *Acta2-CreER*^{T2}*,*

Vhl$^{(flox/flox)}$ mice were exposed to hypoxia for 21 days with or without daily tamoxifen from days 17-21 and then returned to normoxia for 21 days and analyzed (Fig. 3A, B). Tamoxifen-induced *Vhl* deletion in SMCs does not impact reversal of distal muscularization, PH and RVH with re-normoxia (Fig. 3C-E). Taken together, these results refute our initial hypothesis and instead indicate that SMC HIF1-α is not required for the retention of hypoxia-induced distal muscularization and PH.

EC HIFα is sufficient for sustaining hypoxia-induced distal muscularization and PH

In stark contrast to *Vhl* deletion in SMCs, we confirmed previous results (10) that normoxic *Cdh5-CreER*^{T2}*, Vhl*$^{(flox/flox)}$ mice, which have lung ECs with reduced VHL and elevated HIF1-α and HIF2-α (Fig. S5A-C), develop distal arteriole muscularization and extended these findings to demonstrate that these mice develop PH and RVH (Fig. S5D-F). Next, *Cdh5-CreER*^{T2}*, Vhl*$^{(flox/flox)}$ mice were exposed to hypoxia for 21 days with or without tamoxifen (1 mg/day) administration from day 17-21 and then either analyzed at hypoxia day 21 as a control (Fig. S6A) or returned to normoxia for an additional 21 days prior to analysis (Fig. 3A, F). Tamoxifen treatment between hypoxia day 17-21 has no immediate effect on distal muscularization, RVSP or RV weight ratio (Fig. S6B-D). Most importantly, however, despite re-normoxia, tamoxifen-induced mice retain distal arteriole muscularization, PH and RVH (Fig. 3F-I), suggesting that downregulation of EC HIFα is requisite for re-normoxia-induced reversal of these pathological findings.

EC *Hif1a* or *Hif2a* deletion attenuates distal muscularization and PH with continued hypoxia

To complement the EC HIF-α gain-of-function experiments, we next pursued a *Hifa* isoform specific loss-of-function approach. *Cdh5-CreER*^{T2} mice carrying *Hif1a*$^{(flox/flox)}$ or *Hif2a*$^{(flox/flox)}$ were exposed to hypoxia (or normoxia as a control) for 49 days, and tamoxifen (1 mg/day) was or was not administered between hypoxia days 17-21 (Fig. 4A). Tamoxifen-induced EC deletion of either *Hifa* isoform leads to a reversal of distal pulmonary arteriole muscularization, RVSP and RVH despite continued hypoxia (Fig. 4B-I). These results indicate that both HIFα isoforms are required in ECs for retention of hypoxia-induced pathological pulmonary vascular remodeling. As a control, *Cdh5-CreER*^{T2}, *Hif1a*$^{(flox/flox)}$ mice were exposed to normoxia, 17 days of hypoxia or 21 days of hypoxia with concomitant daily tamoxifen injections between days 17-21 (Fig. S6A). The two hypoxic groups showed equivalent distal arteriole muscularization confirming that distal muscularization is essentially complete by day 17 and that *Hif1a* deletion between day 17-21 does not alter the phenotype at day 21 (Fig. S6E). Importantly, in *Cdh5-CreER*^{T2} mice carrying *Hif1a*$^{(flox/flox)}$ or *Hif2a*$^{(flox/flox)}$ and exposed to hypoxia for 31 days, tamoxifen treatment at days 17-21 markedly reduces protein levels of the floxed *Hifa* isoform in lung ECs (Fig. S7).

EC-derived PDGF-B is required for sustaining distal arteriole muscularization

We previously found that hypoxia-induced EC expression of PDGF-B induces distal muscularization and PH and that EC deletion of *Hif1a* attenuates lung PDGF-B levels induced by subsequent hypoxia exposure (10). Tamoxifen treatment at hypoxia days 17-21 markedly reduces levels of the floxed *Hifa* isoform in lung ECs isolated by FACS from *Cdh5-CreER*^{T2} mice also carrying *Hif1a*$^{(flox/flox)}$ or *Hif2a*$^{(flox/flox)}$ at hypoxia day 31 and most importantly downregulates lung EC Pdgfb levels (Fig. 5A-C). Furthermore, whole lung lysates or isolated

lung ECs from wild type mice exposed to hypoxia have upregulated Pdgfb that is reduced with re-exposure to normoxia (Figs. 5D, S8A, B). These data suggest that EC-derived PDGF-B may play a key role in sustaining pathological arteriole remodeling under chronic hypoxia. To evaluate this hypothesis, *Cdh5-CreER*^{T2}*, Pdgfb*$^{(flox/flox)}$ mice were exposed to hypoxia for 31 or 49 days and tamoxifen (1 mg/day) was or was not administered between hypoxia days 17-21 (Figs. 5E, S8C). This tamoxifen treatment induces a marked reduction of lung EC Pdgfb at hypoxia day 31 (Fig. S8D) and of distal muscularization, RVSP and RV weight ratio at day 49 (Fig. 5F-I). Taken together, these findings indicate that an intact and activated EC HIFα-PDGF-B axis is required for retaining pathological distal muscularization and PH under chronic hypoxia.

EC-derived PDGF-B induces SMC Beclin1

PDGF-B treatment of SMCs induces autophagy and cell survival (21, 22). In the lungs of hypoxia- and/or monocrotaline-exposed rats, critical components of the autophagic pathway ATG5, ATG7, Beclin1 and LC3B are markedly increased and p62, which is downregulated during autophagy, is decreased (23, 24, 36). LC3B expression is increased in human PH lung tissues (37). Herein, immunohistochemical staining of lung tissue reveals a marked upregulation of LC3B and Beclin1 and downregulation of p62 in SMCs in PAs of idiopathic PAH (IPAH) patients compared to human controls (Fig. 6; Table S1). Furthermore, mRNA and/or protein quantification (Tables S2, S3) of autophagy-related genes shows similar increases in MAP1LC3B (LC3B) and BECN1 as well as ULK1, ATG5 and ATG7 and downregulation of p62 (Fig. 7A-C). HIF-A isoforms and PDGFB were also up regulated in IPAH lungs compared to controls. These data suggest an activation of autophagy in the human IPAH lung. Next, we examined autophagy during reversal of hypoxia-induced remodeling. *Acta2-CreER*^{T2}*,*

ROSA26R$^{(Zs/+)}$ mice were induced with tamoxifen, rested, exposed to hypoxia for 21 days and then re-normoxia for 10 days. Lung Zs^+ SMCs were isolated by FACS, and the expression of Atg5, Atg7, Becn1 and Map1lc3b is increased with hypoxia and decreased with re-normoxia (Fig. 7D) suggesting a role for autophagy-related genes in the retention of pathological distal arteriole muscularization.

Given the non-cell autonomous inductive effect of EC HIFα/PDGF-B on pathological SMC expansion in chronic hypoxia (10), we next assessed the effects of PDGF-B on autophagy-related genes. PDGF-B treatment of human PASMCs upregulates ATG5, ATG7, BECN1 and MAP1LCB transcripts levels (Fig. S9A), without altering the rate of BECN1 mRNA decay (Fig. S9B), suggesting that BECN1 induction by PDGF-B is not regulated by degradation but instead by transcription. To assess the effects of hypoxia-induced EC conditioned medium on autophagy-related genes in PASMCs, human PAECs were exposed to hypoxia (3% O_2) for 6 or 16 h and then the medium was collected and added to human PASMCs under normoxic conditions for 48 h (Fig. S9C). At both time points, mRNA levels of EC Pdgfb and PASMC ATG7, BECN1 and MAP1LC3B are upregulated (Fig. S9D, E). Furthermore, the hypoxic PAEC-conditioned medium was pre-treated with anti-PDGF-B blocking antibody or IgG isotype control and then added to PASMCs under normoxic conditions for 48 h (Fig. 8A). Transcript levels of ATG7, BECN1 and MAP1LC3B in PASMCs are downregulated with anti-PDGF-B treatment compared to control (Fig. 8B). Thus, these findings suggest that hypoxia-induced EC PDGF-B upregulates autophagy in SMCs.

Beclin1 expression is increased in PAs of mice exposed to hypoxia and is correlated with autophagy in experimental (23, 24) and human PH (see Figs. 6, 7). Herein, *Cdh5-CreER*^{T2}, *Pdgfb*$^{(flox/flox)}$ mice were exposed to hypoxia for 35 days and tamoxifen (1 mg/day) was or was

not administered between hypoxia days 17-21 (Fig. 8C). Tamoxifen-induced *Pdgfb* deletion reduces the percent of Beclin1^{+} distal arteriole SMCs from 51±3% to 18±1% (Fig. 8D, E).

As a therapeutic correlate, we assessed the effects of STI571, which targets the ATP binding site of tyrosine kinases including PDGFRs, on SMC Beclin1 expression. We initially confirmed that STI571 treatment reverses established vascular remodeling in rodent experimental models (38) (Fig. S10). Next, *Acta2-CreER^{T2}, ROSA26R$^{(Zs/+)}$* mice were induced with tamoxifen and exposed to hypoxia for 31 days, and STI571 (0, 50 or 100 mg/kg/d) was administered by daily intraperitoneal injections from hypoxia day 21-31 (Fig. 9A). mRNA levels of Atg5, Atg7, Becn1 and Map1lc3b in lung Zs^{+} SMCs isolated by FACS are significantly decreased in hypoxic mice treated with STI571 compared to no STI571 treatment (Fig. 9B). In addition, immunohistochemical analysis indicates that STI571 treatment markedly reduces percent of distal arteriole SMCs that are Beclin1^{+} in a dose-dependent manner (Fig. 9C, D). Notably, in the more severe pulmonary vascular disease model of combined hypoxia and weekly Sugen 5416 administration (39), STI571 treatment alters mRNA levels of markers of autophagy (decreases) and apoptosis (increases) in lung Zs^{+} SMCs (Fig. S11A-C) and reduces the percent of Beclin1^{+} distal arteriole SMCs (Fig. S11D-F). These results suggest that tyrosine kinase inhibition plays a role previously not described of reducing SMC autophagy to reverse established distal arteriole muscularization.

SMC Beclin1 is required for the retention of distal arteriole muscularization and PH

Thus far we have shown that the EC HIFα-PDGF-B axis is important for sustaining established distal arteriole muscularization under continuous hypoxia and that EC-derived PDGF-B induces expression of SMC Beclin1 and other autophagy genes. To evaluate the

specific role of SMC Beclin1 in sustaining pulmonary vascular remodeling and PH, *Acta2-CreER^{T2}, Becn1$^{(flox/flox)}$* mice were treated with hypoxia for 35 or 49 days, and tamoxifen was or was not administered between hypoxia days 17-21 (Figs. 10A, S12A). This tamoxifen treatment induces a marked reduction in the percent of distal arterioles SMCs that are Beclin1^{+} at day 35 (Fig. S12B, C) and by day 49, reverses hypoxia-induced distal muscularization, PH and RVH (Fig. 10B-E). Additionally, mice of the same genotype were exposed to hypoxia for 49 days with injections of Sugen 5416 at day 0, 7 and 14, and tamoxifen was or was not administered between hypoxia days 17-21 (Fig. 10F). Similar to the hypoxia model (Fig. 10A-E), with Sugen 5416/hypoxia treatment, deletion of *Becn1* in SMCs reverses established distal arteriole muscularization, PH and RVH (Fig. 10G-J). In contrast, *Becn1* deletion in ECs does not alter pulmonary vascular remodeling in mice exposed to chronic hypoxia (Fig. S13). Thus, Beclin1 in SMCs, but not ECs, is requisite for sustaining pathological distal muscularization and PH.

Cross talk between autophagy and apoptosis is regulated by Beclin1. For instance, as the binding partner for the anti-apoptotic mediator Bcl2, Beclin1 is critical as to whether cells are resistant to apoptosis or autophagy (40). Beclin1-deficient mice display embryonic lethality and neuronal apoptosis, suggesting that Beclin1 is associated with cell survival (41, 42). Herein, *Acta2-CreER^{T2}, Becn1$^{(flox/flox)}$* mice were treated with hypoxia for 35 days, and tamoxifen was or was not administered between hypoxia days 17-21 (Fig. S14A). *Becn1* deletion in SMCs reduces the percent of distal arteriole SMCs that are ATG7^{+} by more than 50% (Fig. S14B, C). We next used *Acta2-CreER^{T2}, ROSA26R$^{(Zs/+)}$* mice carrying *Becn1$^{(flox/flox)}$* or *Becn1$^{(+/+)}$* to evaluate the effect of *Becn1* deletion in SMCs on hypoxia-induced Atg5 and Atg7 expression. These mice were treated with hypoxia for 35 days, and tamoxifen was administered between hypoxia days

17-21 (Fig. 11A). *Becn1* deletion attenuates the hypoxia-induced increase in Atg5 and Atg7 transcript levels (Fig. 11B).

Finally, the effect of *Becn1* deletion in SMCs on apoptosis and cell proliferation was analyzed. *Acta2-CreER*^{T2}*, ROSA26R*$^{(Zs/+)}$ mice carrying *Becn1*$^{(flox/flox)}$ or *Becn1*$^{(+/+)}$ were treated with hypoxia for 35 days, and tamoxifen was administered between hypoxia days 17-21 (Figs. 12A, S15A). Lung Zs^{+} SMCs were isolated by FACS and subjected to qRT-PCR for transcripts of pro-apoptotic genes Bax, Puma, Noxa, Bim, and Apaf1, the pro-proliferative gene Ccna and anti-proliferative genes p21 and p27. Tamoxifen-induced *Becn1* deletion leads to a significant increase in levels of the pro-apoptotic and anti-proliferative mRNAs and reduction of Ccna mRNA with hypoxia (Figs. 12B, S15B). Additionally, *Acta2-CreER*^{T2}*, Becn1*$^{(flox/flox)}$ mice were treated with hypoxia for 35 days, and tamoxifen was or was not administered between hypoxia days 17-21. Immunohistochemistry indicates that *Becn1* deletion results in a ~6.5-fold or ~2.5-fold increase in the percent of distal arteriole SMCs that stain with antibodies against total BAX or activated (6A7) BAX (Fig. 13A-D), respectively, suggesting that *Becn1* deficiency in SMCs induces cell death to reverse established distal arteriole muscularization. As a confirmation, tamoxifen treatment of *Acta2-CreER*^{T2}*, Becn1*$^{(flox/flox)}$ mice increases the percent of TUNEL^{+} distal arteriole SMCs by ~8-fold (Fig. 13E, F). Additionally, immunohistochemistry indicates that *Becn1* deletion decreases the percent of distal pulmonary arteriole SMCs that express Ki67 (Fig. S15C, D). Taken together, these data suggest that *Becn1* deletion in SMCs reverses hypoxia-induced distal arteriole muscularization by promoting SMC apoptotic cell death and decreasing proliferation.

Discussion

Excess SMCs are a critical component of many cardiovascular diseases, including SMC coating of normally unmuscularized distal pulmonary arterioles in PH. Mechanisms governing how pathological hypermuscularization is sustained are poorly understood. In this study, we leverage the reversal of hypoxia-induced distal muscularization that occurs with re-normoxia to delineate how pathological distal arteriole muscularization is retained in hypoxia-induced PH and how it can be attenuated. With normoxia after hypoxia exposure, our findings demonstrate sequential regression of distal pulmonary arteriole muscularization, PH and RVH in mice, starting at day 14 of re-normoxia (Fig. 1). The distal arteriole SMCs do not change fates with re-normoxia but rather undergo apoptosis, which is in agreement with prior studies of re-normoxia in rats showing apoptosis of SMCs surrounding small arterioles (7, 8). Interestingly, we found that hypoxia induces distal muscularization despite a prior hypoxia and re-normoxia cycle, suggesting that a re-normoxia phase does not inhibit mechanisms underlying pathological muscularization. Another key finding is that the SMC loss with re-normoxia is limited to the distal arteriole region, suggesting that distal arteriole SMCs which primarily derive from PDGFR-β^+SMA$^+$SMMHC$^+$ progenitors (28) differ from SMCs in the more proximal regions of the arteriole in terms of sensitivity to re-normoxia. The nature of this sensitivity is not known but warrants further analysis as it potentially has profound clinical ramifications.

Targeting HIF-1α or HIF-2α pharmacologically or genetically reduces chronic hypoxia-induced vascular remodeling (10, 12-15, 43-47). Although there are some discrepancies, during the adult onset of hypoxia-induced pulmonary vascular remodeling and PH, a pathological role of HIF2-α in ECs is generally more established than that of HIF1-α whereas in SMCs, HIF1-α may contribute. Tamoxifen-induction of *Hif1a*$^{(flox/flox)}$ mice also carrying *Pdgrb-CreER*^{T2} [marking pericytes, fibroblasts and SMC progenitors in the lung (48)] or *Myh11-CreER*^{T2}

attenuates hypoxia-induced pulmonary vascular disease (10, 14). In contrast, constitutive *Hif1a* deletion in SM22α^{+} cells increases pulmonary artery pressure under normoxia and hypoxia (46). Our findings indicate that SMC HIF1-α is neither necessary nor sufficient to retain established distal pulmonary arteriole muscularization in hypoxia-induced PH (Figs. 3, S3). EC deletion of *Hif2a*, but not *Hif1a*, with *L1-Cre* or *Tie2-CreER^{T2}* attenuates hypoxia-induced pulmonary vascular disease (15, 47). In contrast, *Cdh5-CreER^{T2}*, *Hif1a$^{(flox/flox)}$* are protected against hypoxia-induced distal pulmonary arteriole muscularization and PH (10).

Compared to the roles of vascular cell-specific HIFα isoforms in induction of pulmonary vascular disease, their roles in sustaining pathological SMCs in PH is understudied and poorly understood. In the current study, although we do not directly compare the relative effects of EC HIF1-α and HIF2-α in retention and reversibility of established pulmonary vascular disease, our results suggest that with *Cdh5-CreER^{T2}*, deletion of *Hif2a* reduces distal muscularization (by ~87%) more so than *Hif1a* deletion does (by ~62%) despite continued hypoxia (Fig. 4). Furthermore, EC deletion of *Hif2a* restores pulmonary artery pressure and the RV weight ratio to normoxic levels whereas *Hif1a* EC deletion significantly reduces these hemodynamic parameters, but not to normoxic levels. As a complementary approach, studies with *Cdh5-CreER^{T2}, Vhl$^{(flox/flox)}$* mice, which have elevated EC HIFα levels under normoxia (10), indicate that EC HIFα induces the retention of pathological muscularization. Indeed, when these mice are injected with tamoxifen at the tail end of a 21 day hypoxia exposure and then returned to normoxia, distal arteriole muscularization, PH and RVH persists (Fig. 3). These results highlight that sustaining pathological distal muscularization is not a passive cell intrinsic phenomenon of SMCs but instead requires input from ECs.

Signaling by PDGF-B through PDGFR-β is central to PH pathogenesis. In the lung, PDGF-B is primarily synthesized by and released from ECs and circulating inflammatory cells, and increased levels of PDGF-B are reported in the blood and lung tissue of patients with PH (29, 49-52). In mice, lung EC Pdgfb levels are elevated by day 7 of hypoxia (10) and remain upregulated at day 31 compared to normoxia (Fig. 5). Analysis of $CD64^{+}Ly6G^{-}$ macrophages in bronchoalveolar lavage fluid as well as in the residual lung (i.e., after removal of this fluid) from mice exposed to hypoxia shows that Pdgfb increases within 1 day of hypoxia and, in the case of the residual lung, peaks at day 3 (29). Hypoxia-induced distal muscularization is completely prevented in *Pdgfb*$^{(+/-)}$ mice and markedly attenuated by deletion of *Pdgfb* specifically in ECs or monocytes/macrophages (10, 28, 29). Herein, we demonstrate that deletion of EC *Pdgfb* in chronic hypoxia reverses established distal arteriole muscularization and PH (Fig. 5). In contrast, reduction of lung macrophage Pdgfb levels does not reverse established distal arteriole muscularization (29). Taken together, these findings suggest that macrophage-derived PDGF-B may be primarily involved in the initial induction of hypoxia-mediated distal muscularization whereas EC PDGF-B is critical in both the initiation and maintenance of distal muscularization.

It is interesting to compare these results to the role of the PDGF pathway in sustaining SMC-derived cells in atherosclerosis. Indeed, in *Apoe*$^{(-/-)}$ mice with established Western diet-induced atherosclerosis, *Pdgfrb* deletion with *Myh11-CreER*^{T2} reduces fibrous cap SMA^{+} cells that are marked by the *Myh11-CreER*^{T2} lineage by 50% without altering the total number of SMA^{+} cells in the fibrous cap (53). Taken together, the findings suggest that when *Pdgfrb* is deleted in differentiated SMCs, a distinct population of cells contributes to retention of the atherosclerotic fibrous cap whereas with *Pdgfb* deletion in ECs during PH of chronic hypoxia, pathological SMCs are lost and not replaced.

PDGF-B treatment of cultured SMCs induces autophagy, as assessed by autophagosome formation and expression of ATG5, ATG7, Beclin1 and LC3B, promoting cell survival (21, 22). Autophagy is a catabolic process that is essential to cellular homeostasis under stress as it facilitates recycling of superfluous or dysfunctional organelles via lysosomal degradation (54). In human IPAH, LC3B is upregulated in lung lysates and large and small vessels of the lung (37). Our data from PAs of IPAH patients indicate that Beclin1 and LC3B are increased in EC and SMC layers and p62 is downregulated in SMCs (Figs. 6, 7). Furthermore, in addition to BECN1 and MAP1LC3B, we found that transcript levels of ULK1, ATG5, ATG7 as well as HIFA and PDGF-B are also upregulated in IPAH lung lysates. In diverse experimental rodent PH models, other groups have demonstrated autophagy is enhanced in lung ECs, SMCs and PAs (23, 24, 36, 37, 55). Herein, lung SMC levels of autophagy-related gene products, including Becn1, are demonstrated to be increased with hypoxia and downregulated with re-normoxia, suggesting that autophagy may be integral to retention of hypoxia-induced distal muscularization. Furthermore, data from culturing SMCs with conditioned medium from hypoxic ECs and in vivo studies of EC-specific deletion of *Pdgfb* or STI571 treatment suggest that under hypoxia with or without concomitant Sugen 5416, EC-derived PDGF-B induces autophagy-related transcripts in SMCs and specifically Beclin1 protein in distal pulmonary arteriole SMCs via a tyrosine kinase (most likely PDGFR-β) (Figs. 8, 9, S11). These data suggest that hypoxia-mediated EC PDGF-B non-cell autonomously induces Beclin1 in pathological distal SMCs and perhaps, thereby promotes cell survival.

Beclin1 is a key member of a complex that is integral to major events during the autophagic process ranging from formation of the autophagasome to autophagasome/endosome maturation (56). Beclin1 deficiency leads to defective autophagy, and *Becn1* null embryos die by

E7.5 with widespread cell death (25, 42). Our results indicate that SMC-specific deletion of *Becn1* reduces expression of ATG7 in distal pulmonary arteriole SMCs during chronic hypoxia and reverses distal muscularization and PH established by exposure to hypoxia +/- Sugen 5416 whereas no effect was observed with *Becn1* deletion in ECs (Figs. 10, 11, S13, S14). Notably, the lysosomal inhibitor chloroquine attenuates autophagy and degradation of bone morphogenetic protein type II receptor, a key player in human PAH, and has been shown to reverse pulmonary vascular remodeling and hemodynamics in monocrotaline or hypoxia-induced PH in rats (23, 36). An important study in the field assessed the role of autophagy in inducing PH using mice with deletions of autophagy genes (37). Mice with global deletion of the *Map1lc3b* gene were shown to have exacerbated hypoxia-induced pulmonary arteriole wall thickening, PH and RVH (37). This protective effect may be specific to LC3B as *Becn1*$^{(+/-)}$ mice do not share a similar protection in response to hypoxia (37). In contrast, in a myocardial ischemia-reperfusion model, autophagy is elevated, and *Becn1*$^{(+/-)}$ mice have reduced autophagasome formation and myocardial injury (57). Thus, depending on the cardiovascular disease model, pathobiological effects of specific autophagic proteins differ.

The complex and intimate relationship between autophagy and apoptosis is critical to the pathophysiology of PH (36, 56, 58). Beclin1 plays an important role in cell survival and death, and although a number of pathways have been implicated to underlie its anti-apoptotic effects in diverse tissues, a common mechanism is not established. Beclin-1 is a regulator of the Bcl2 family of proteins, which includes key pro-apoptotic (e.g., Bax, Puma, Noxa, Bim) and anti-apoptotic (e.g., Bcl-2) mediators (40, 56, 59), and is required for ATG5/ATG7-dependent autophagy. Knockdown of Atg5 in PASMCs inhibits autophagy and proliferation and induces apoptosis (36, 56). Interestingly, deletion of *Becn1* in cortical and hippocampal neurons leads to

enhanced activated caspase 3, suggestive of apoptosis, and severe neurodegeneration, concomitant with perturbations in both late endosome formation and phospholipid localization (41). In *C. elegans*, BEC-1, the orthologue of mammalian Beclin1, forms a complex with the anti-apoptotic protein CED-9/Bcl-2, and BEC-1 depletion triggers caspase-dependent programmed cell death (60). Additionally, mice with *Becn1* deletion in adipocytes develop lipodystrophy and have elevated endoplasmic reticulum stress gene expression stimulating adipocyte apoptosis (61). Herein, following the establishment of hypoxia-induced pulmonary vascular remodeling, tamoxifen injection of *Acta2-CreER*^{T2}, *Becn1*$^{(flox/flox)}$ mice reduces the level of autophagy markers and induces pro-apoptotic genes in lung SMCs (Figs. 11, 12). In distal arteriole SMCs, this treatment decreases ATG7 expression and increases levels of total and activated BAX and apoptosis (Figs. 13, S14), indicating that Beclin1 in SMCs prevents programmed cell death of established distal SMCs. Taken together, our studies support a model in which chronic hypoxia upregulates EC HIFα and thus, PDGF-B. In turn, PDGF-B induces SMC Beclin1 expression to promote the retention of established pulmonary distal arteriole SMCs, PH and RVH, whereas re-normoxia reverses these processes. These findings pave the way for novel therapeutic strategies aimed at reversing established hypermuscularization and PH.

Methods

Sex as a biological variable

As indicated in the figure legends, male and female mice were used in the studies.

Animals and tamoxifen treatment

All animal procedures were approved by the Institutional Animal Care and Use Committee at Yale University. Wild type mice were of a C57BL/6 background. The mouse strains used were *Acta2-CreER*^{T2} (62), *Cdh5-CreER*^{T2} (63), *Bmx-CreER*^{T2} (31), *ROSA26R*$^{(mTmG/mTmG)}$ (64), *ROSA26R*$^{(ZsGreen1/ZsGreen1)}$ (65), *Pdgfb*$^{(flox/flox)}$ (66), *Vhl*$^{(flox/flox)}$ (67), *Hif1a*$^{(flox/flox)}$ (68), *Hif2a*$^{(flox/flox)}$ (69) and *Beclin1*$^{(flox/flox)}$ (41). Male and female mice aged 2-4 months and sex- and age-matched controls were used. Mice were exposed to hypoxia (FiO_2 10%) or normoxia for up to 49 days and then re-exposed to normoxia for up to 42 days. In select experiments, mice were again re-exposed to 21 days of hypoxia. For CreER-catalyzed recombination, mice were injected intraperitoneally with tamoxifen at 1 mg/day for 5 days, rested for 5 days and then exposed to normoxia or hypoxia. In select experiments, mice were injected with tamoxifen (1 mg/day) during hypoxia days 17–21. For studies of more severe pulmonary vascular disease, during hypoxia exposure, mice were subcutaneously injected with Sugen 5416 (20 mg/kg/dose, Millipore-Sigma, S8442) on hypoxia days 0, 7 and 14.

Hypoxia treatment and hemodynamic measurements

Mice were exposed to hypoxia (FiO2 10%) in a rodent hypoxia chamber equipped with a calibrated oxygen controller and sensor (BioSpherix). Right ventricular systolic pressure was measured by inserting a catheter (Millar Instruments) into the right ventricle via the right jugular

vein. Subsequently, mice were sacrificed, and the heart was dissected with the weight ratio of the right ventricle to the sum of the left ventricle and septum assessed as previously described (27).

STI571 (Imatinib mesylate) administration

Acta2-CreER^{T2}*, ROSA26R*$^{(Zs/+)}$ mice were injected with tamoxifen, rested and exposed to normoxia or hypoxia for 31 days. Starting at hypoxia day 21, mice received daily intraperitoneal injections of STI571 (Selleckchem, S1026) at a dose of 50-100 mg/kg suspended in 0.9% sterile saline for 10 days as previously described (38).

Lung preparation for immunohistochemistry

Lungs were prepared for immunohistochemistry as described previously (27). Briefly, mice were euthanized by isoflurane inhalation, and PBS was infused into the right ventricle until the lungs turned a white color to flush the pulmonary vasculature. Lungs were then inflated with 2% low-melt agarose and incubated in ice-cold PBS for 30 min. Solidified agarose-filled lobes were immersed in Dent's fixative (4:1, methanol:dimethyl sulfoxide) at 4°C overnight and then washed and stored in 100% methanol at -20°C. Lungs were bleached by incubating with 5% H_2O_2 in methanol for 10 min, sequentially rehydrated into PBS and vibratome-sectioned at a thickness of 150 µm.

Immunohistochemistry

Vibratome lung sections were incubated with blocking buffer (5% normal goat serum in 0.5% Triton X-100/PBS [PBS-T]) at 4°C overnight. Sections were exposed to primary antibodies in blocking buffer for 1-3 days at 4°C, washed 3 times in PBS-T and incubated in secondary

antibodies overnight at 4°C. Sections were then washed 6 times in PBS-T and placed on slides in mounting media (Dako, S3023). Primary antibodies used were rat anti-MECA-32 (1:15, Developmental Studies Hybridoma Bank [DSHB, AB-531797]), rabbit anti-GFP (1:100, Invitrogen, A11122), rabbit anti-Beclin1 (1:100, Abcam, ab217179), rabbit anti-ATG7 (1:100, Abcam, ab133528), rabbit anti-BAX (1:100, Abcam, ab32503), BAX (6A7) Alexa Fluor 546 (1:100, Santa Cruz, sc-23959) and/or anti-SMA directly conjugated to Cy3 or FITC (1:250, Sigma-Aldrich, C6198 or F3777, respectively). Secondary antibodies were conjugated to Alexa 488, Alexa 546 and Alexa 647 (1:250, Invitrogen, A11008, A11010 and A21247, respectively). Nuclei were stained with DAPI (1:500, Sigma-Aldrich, D9542). TUNEL assay was performed as per the *In Situ Cell Death Detection, TMR red* protocol (Roche Diagnostics, 12156792910).

As in prior studies (10, 27-29), immunohistochemical analysis focused on three vascular beds located in the cranial and medial aspects of the adult left lung and categorized arteriole segments in each of these vascular beds (by both position in the vascular tree and lumen diameter) as proximal (>75 μm diameter), middle (25-75 μm diameter) or distal (<25 μm diameter). The arteriole beds studied are in proximity to airway branches L.L1.A1.M1, L.L1.A1.L1 and L.L2.M2 (L, left main bronchus; L1, L2, L3 lateral branches; M1, M2, medial branches; A1, A2, anterior branch; Fig. S1A). Distal arterioles in these regions are reproducibly unmuscularized under basal conditions and become muscularized with hypoxia (10, 27-29). Muscularization of distal arterioles was quantified as the ratio of length of SMC coverage of the distal arteriole (from the middle-distal [M-D] arteriole border to the most distal SMA staining) to the entire length of the distal arteriole (from the M-D border to the capillary front; maximum distal arteriole length quantified was 300 μm).

Human lung samples from de-identified patients with IPAH and controls were obtained from the (PHBI; Table S1). Frozen OCT embedded tissues were sectioned, and sections were fixed in 4% paraformaldehyde for 15 min at room temperature, washed 3 times in PBS, permeabilized with PBS-T for 10 min and immunostained. Sections were incubated in primary antibodies diluted in blocking buffer overnight at 4°C, washed 3 times in PBS-T and incubated in secondary antibodies for 1 h at room temperature. Primary antibodies used were mouse anti-LC3B (1:100, Abcam, ab232940), mouse anti-Beclin1 (1:100, Abcam, ab114071), mouse anti-p62 (1:100, Abcam, ab56416), rabbit anti-ATG7 (1:100, Abcam, ab133528), rabbit anti-Cx40 (1:100, Abcam, 213688) and/or anti-SMA directly conjugated to Cy3 or FITC (1:250, Sigma-Aldrich , C6198 or F3777, respectively). Secondary antibodies were conjugated to Alexa 488 and Alexa 568 (1:250, Invitrogen, A11029 or A11031). Nuclei were stained with DAPI (1:500).

Murine lung EC and SMC isolation

The lung vasculature was flushed with PBS as noted above, and lobes were carefully dissected from bronchi and mediastinal connective tissue. Lobes were finely minced and digested using the lung dissociation kit (Miltenyi Biotec, 130-095-927), mechanically dissociated with gentleMACS™ Dissociator (Miltenyi Biotec), filtered through a 70 µm cell strainer and centrifuged for 5 min at 4°C. In preparation for isolation of ECs or SMCs by FACS and RNA analysis by qRT-PCR, the cell pellet was resuspended in 5% fetal bovine serum (FBS) in PBS to generate a single cell suspension. For EC isolation, the single cell suspension was incubated with anti-CD31-APC (1:200, BD Pharmingen, 551262) and anti-CD45-Pacific blue (1:200, Biolegend, 103126) antibodies for 30 min at 4°C. Cells were washed and resuspended in PBS with 1% FBS and propidium iodide (PI) was used as a viability dye (1:1000, Sigma-Aldrich ,

P4864). $CD31^{+}CD45^{-}PI^{-}$ cells were sorted on a BD FACSAria II cell sorter. For SMC isolation, *Acta2-CreER*^{T2}, *ROSA26R*$^{(Zs/+)}$ mice carrying were induced with tamoxifen (1 mg/day for 5 days), and a single cell suspension was obtained. Cells were stained with PI, and FACS was used to isolate $Zs^{+}PI^{-}$ cells. For Western blot analysis, lung ECs were isolated with anti-CD31-coated magnetic beads as previously described (10). Briefly, sheep anti-rat-IgG Dynal magnetic beads (Invitrogen, 11035) were resuspended in PBS containing 0.1% FBS and incubated with rat anti-CD31 monoclonal antibody (1:250, BD Biosciences) overnight at 4°C. Beads were then washed and stored at 4°C. Lung single cell suspensions in PBS containing 0.1% FBS were incubated with these anti-CD31-coated beads for 20 min at room temperature and washed four times with PBS. A magnet was used to separate cells bound to beads from unbound cells.

Cell culture and hypoxia

Human PASMCs and PAECs (American Type Culture Collection, PCS-100-023 and PCS-100-022, respectively) were cultured for up to six passages in SmGM™ 2 Smooth Muscle Cell Growth Medium-2 BulletKit™ (CC-3182) and EGM™ 2 Endothelial Cell Growth Medium-2 BulletKit™(CC-3162), respectively. PASMCs were or were not treated with 20 ng/ml recombinant PDGF-B (Sigma) for 24 h, and mRNA levels were determined by qRT-PCR. For mRNA decay assays, PASMCs were similarly cultured with PDGF-B or vehicle (DEPC water). Cells were then treated with 50 μmol/L of transcription inhibitor 5,6-dichloro-1-beta-D-ribofuranosyl-benzimidazole (DRB; Sigma-Aldrich, D1916) and collected at 0, 1.5, 3, 6, 12, and 24 h after initiation of DRB treatment for qRT-PCR analysis. For conditioned medium experiments, PAECs were subjected to either normoxia or 3% hypoxia for 6 or 16 h at 37°C, and then, in select studies, treated with 20 μg/ml IgG isotype control or anti-PDGF-B blocking

antibody (R&D Systems, AB-108-C or AF-220-NA, respectively) for 1 h. The PAEC conditioned medium was added to normoxic PASMCs for 48 h. Cells were collected for qRT-PCR analysis.

Quantitative real time RT-PCR analysis

RNA from murine lung samples was isolated with the RNeasy Plus Kit (Life Technologies) and reverse transcribed with the iScript cDNA Synthesis Kit (Bio-Rad). RNA lung samples from patients with IPAH and controls were obtained from the PHBI for qRT-PCR analysis (Table S2). Transcript levels were determined by qRT-PCR and normalized to 18S. Forward and reverse primer are listed in Table S4.

Western Blot

Lysates were prepared by mechanical homogenization of mouse lungs in lysis buffer (RIPA buffer and protease inhibitor cocktail) on ice with a glass pestle tissue homogenizer (Pyrex) or by suspension of EC-bound beads in lysis buffer. Lysates were centrifuged at 12,000g at 4°C for 5 min, supernatants were collected, and protein concentration was determined by BCA assay (Thermo Fisher Scientific). Protein samples were resolved by 7-15% SDS-PAGE, transferred to Immobilon PVDF membranes (Millipore), blocked with 5% nonfat dry milk, washed in 0.1% Tween 20/TBS, and probed with primary antibodies overnight at 4°C. Membranes were incubated with HRP-conjugated secondary antibodies (Dako), washed in 0.1% Tween 20/TBS, developed with Supersignal West Pico Maximum Sensitivity Substrate (Pierce), and analyzed with the G:BOX imaging system (Syngene). Primary antibodies used for Western blot analysis were rabbit anti-HIF1-α (1:500, Novus, NB100-449), rabbit anti-HIF2-α (1:500,

Novus, NB100-122), rabbit anti-Beclin1 (1:500, Novus, NB110-87318), rabbit anti-LC3B (1:500, Cell Signaling Technology, 2775), rabbit anti-p62 (1:500, Abcam, ab109012).

Imaging

Lung sections were imaged on confocal microscopes (PerkinElmer UltraView VOX spinning disc or Leica SP5 point scanning). Volocity software (PerkinElmer) and Adobe Photoshop was used to process images.

Statistics

All data are presented as mean ± SD. Student's t test and multi-factor ANOVA with Tukey's multiple comparisons test were used to analyze the data (GraphPad Prism software, v7). The statistical significance threshold was set at $p < 0.05$. All tests assumed normal distribution and were two-sided.

Study Approval

All mouse experiments were approved by the IACUC at Yale University. De-identified human tissues were obtained from the Pulmonary Hypertension Breakthrough Initiative in accordance with the Institutional Review Boards of Yale University (IRB# 1005006865). All experiments were performed in accordance with relevant ethical guidelines.

Data and materials availability

All data associated with this study are present in the paper or the Supplementary Information, and data values are included in the Supporting Data Values file. Reagents and materials associated with this study are available from the corresponding author (D.M.G.).

Author contributions

All authors conceived of and designed experiments. F.Z.S., A.K. and J.S. performed them. All authors analyzed the results, prepared the figures and wrote and revised the manuscript.

Acknowledgements

We thank Greif laboratory members for input. F.Z.S. was supported by a Brown-Coxe Fellowship from Yale University and a postdoctoral fellowship from the American Heart Association (AHA; 18POST34070007). J.S. was supported by the Overseas Research Fellowship from the Japan Society for the Promotion of Science (no. 202260284) and the AHA/Children's Heart Foundation Congenital Heart Defect Research Award (23POSTCHF1022933). Funding was also provided by the NIH (R35HL150766, R01HL125815, R01HL142674, R01HD110059, R21AG062202, R21NS123469 to D.M.G.) and AHA (Established Investigator Award, 19EIA34660321 to D.M.G.).

Wild type

A

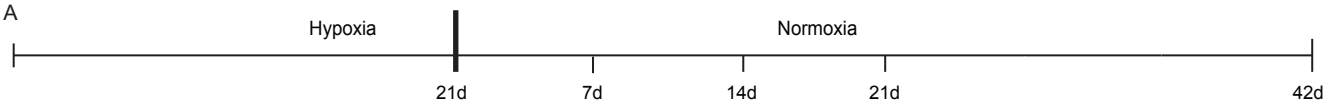

B

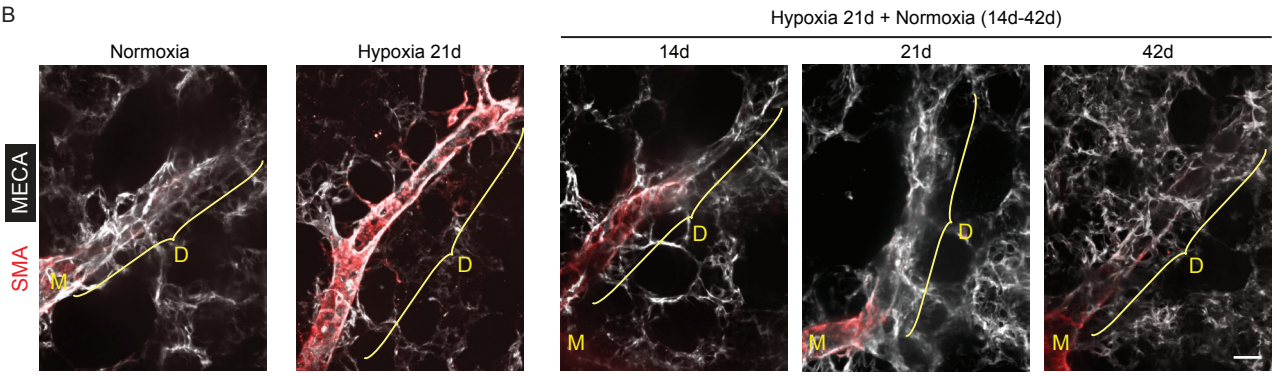

C

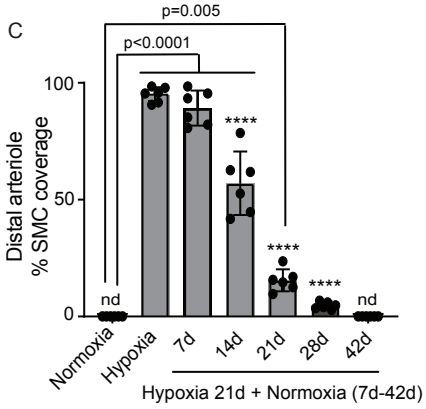

D

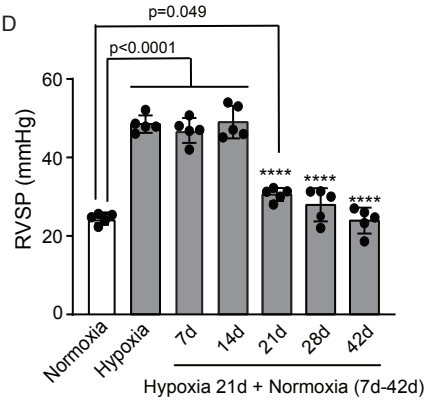

E

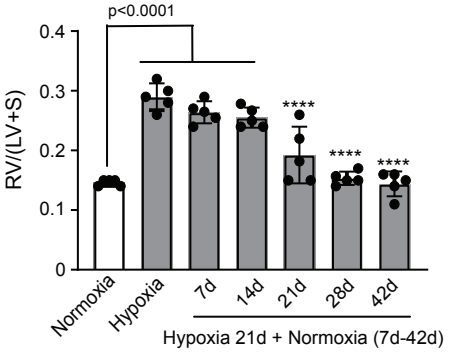

F

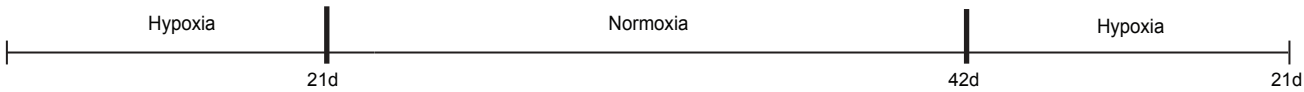

G

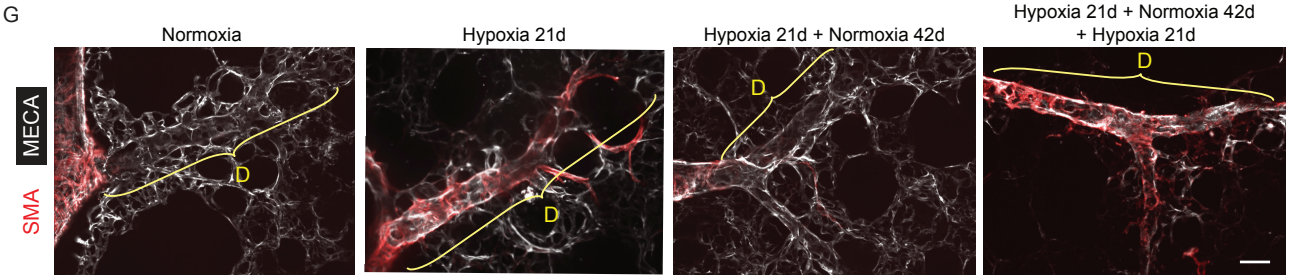

Normoxia | Hypoxia 21d | Hypoxia 21d + Normoxia 42d | Hypoxia 21d + Normoxia 42d + Hypoxia 21d

H

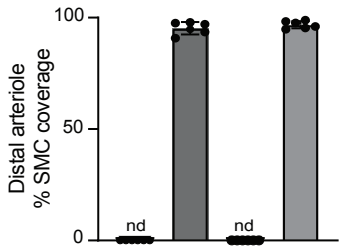

I

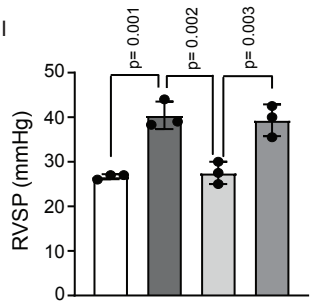

J

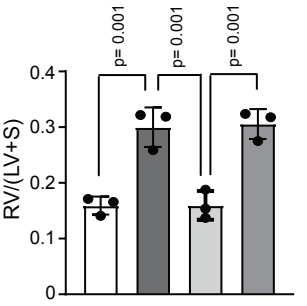

Figure 1. Reversal of distal arteriole muscularization with re-normoxia following hypoxia. **A,** Experimental strategy for (B-E). **B-E,** Wild type mice were maintained in normoxia or were exposed to hypoxia for 21 days and either analyzed at that point or following re-exposure to normoxia for 7-42 days as indicated. In (B), vibratome lung sections were stained for SMA and the EC marker MECA-32. M and D, middle and distal arterioles are indicated, respectively. In (C), percent of distal arterioles covered by SMCs, in (D), RVSP (right ventricle systolic pressure; equivalent to PA systolic pressure) and in (E), the RV weight ratio (weight of the right ventricle [RV] divided by the sum of left ventricle [LV] and septum [S] weight) were measured. n=5-6 mice (3 males, 2-3 females) per experimental group and 3 arterioles per mouse. nd, not detected; multi-factor ANOVA with Tukey's multiple comparison test, ****, $p<0.0001$ vs. hypoxia. **F,** Experimental strategy for (G-J). **G-J,** Wild type mice were exposed to either: i) normoxia; ii) hypoxia 21 days; iii) hypoxia 21 days followed by normoxia 42 days; or iv) hypoxia 21 days, normoxia 42 days and hypoxia again for 21 days. Vibratome lung sections were stained for SMA and MECA-32 in (G). Percentage of distal arteriole covered by SMCs, RVSP and RV/(LV+S) were measured in (H-J). n=3 mice (1 male, 2 females); multi-factor ANOVA with Tukey's multiple comparison test. nd, not detected. Scale bars, 20 μm.

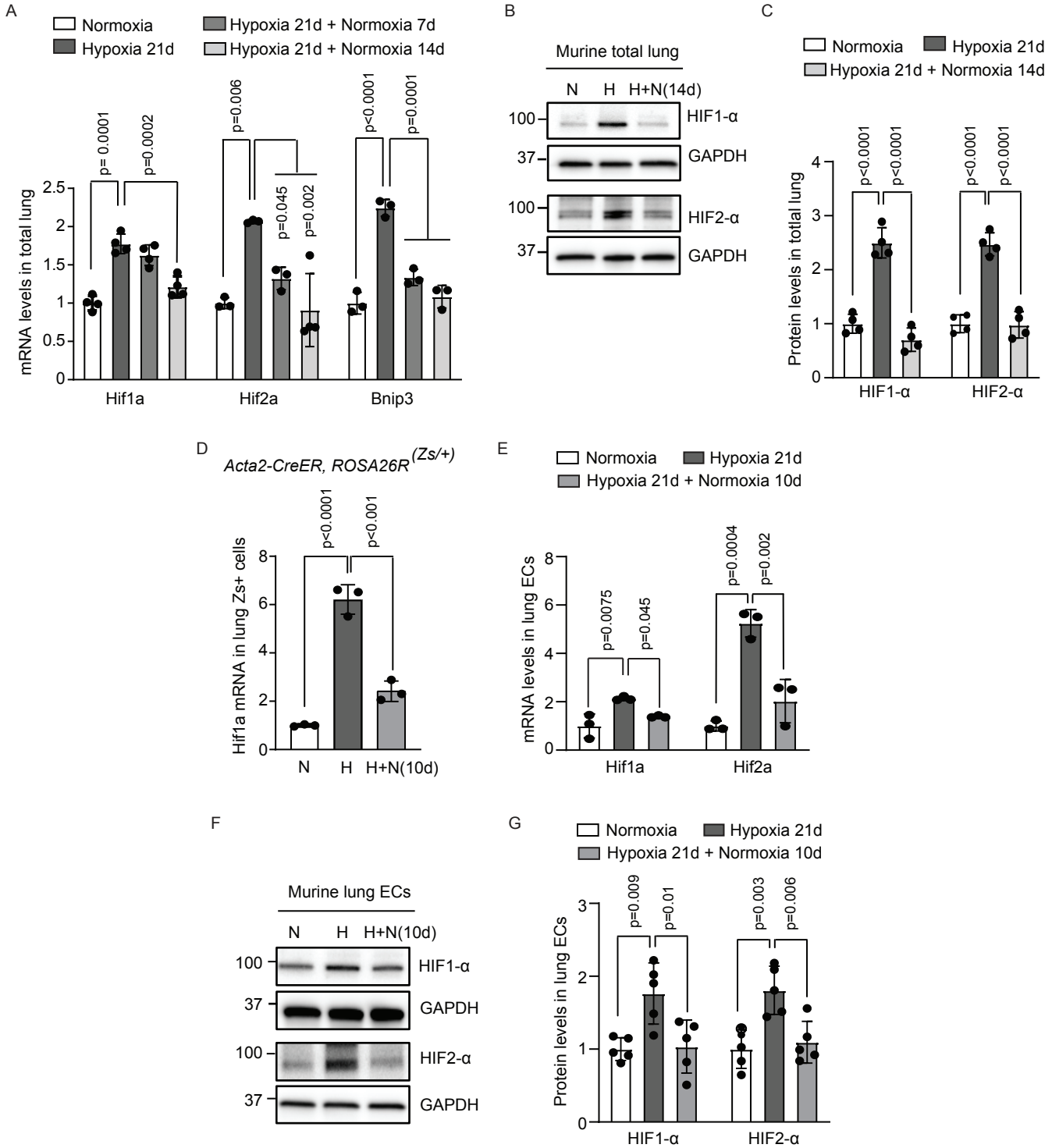
A
Normoxia
Hypoxia 21d
Hypoxia 21d + Normoxia 7d
Hypoxia 21d + Normoxia 14d
mRNA levels in total lung
p= 0.0001
p=0.0002
p=0.006
p=0.045
p=0.002
p<0.0001
p=0.0001
Hif1a
Hif2a
Bnip3
B
Murine total lung
N
H
H+N(14d)
HIF1-α
GAPDH
HIF2-α
C
Protein levels in total lung
p<0.0001
HIF1-α
HIF2-α
D
Acta2-CreER, ROSA26R(Zs/+)
Hif1a mRNA in lung Zs+ cells
p<0.0001
p<0.001
H+N(10d)
E
Hypoxia 21d + Normoxia 10d
mRNA levels in lung ECs
p=0.0075
p=0.045
p=0.0004
p=0.002
F
Murine lung ECs
G
Protein levels in lung ECs
p=0.009
p=0.01
p=0.003
p=0.006

Figure 2. HIFα is upregulated with hypoxia and downregulated with re-normoxia. A, Wild type mice were exposed to either normoxia or hypoxia for 21 days with or without subsequent re-normoxia for 7 or 14 days. Lung lysates were subjected to qRT-PCR to assess Hif1a, Hif2a and Bnip3 levels. n=3-4 mice (2 males, 1-2 females) per experimental group. **B, C,** Wild type mice were exposed to normoxia or hypoxia for 21 days and then were or were not subjected to normoxia for 14 days. Whole lung lysates were subjected to Western blot for HIF1-α, HIF2-α and GAPDH protein (B) with densitometry relative to GAPDH and normalized to normoxia (C). n=4 mice (2 males, 2 females) per experimental group. **D,** *Acta2-CreER*^{T2}*, ROSA26R*$^{(Zs/+)}$ mice were induced with tamoxifen (1 mg/day for 5 days), rested for 5 days, exposed to hypoxia for 21 days and then re-normoxia for 10 days. Zs^{+} cells were isolated by FACS, and Hif1a expression level was measured by qRT-PCR. n=3 mice (1 male, 2 females) per experimental group. **E-G,** Wild type mice were exposed to normoxia or hypoxia for 21 days followed by normoxia for 10 days. In (E), lung $CD31^{+}CD45^{-}$ ECs were isolated by FACS, and transcript levels of Hif1a and Hif2a were measured with qRT-PCR. n=3 (1 male, 2 females) per experimental group. In (F, G), lung ECs were isolated with anti-CD31-coated beads. Western blot analysis of EC lysates for HIF1-α, HIF2-α and GAPDH protein are shown (F) with densitometry relative to GAPDH and normalized to normoxia (G). n=5 mice (2 males, 3 females) per experimental group. Multi-factor ANOVA with Tukey's multiple comparison test was used (A, C-E, G). N, normoxia; H, hypoxia; H+N, hypoxia followed by normoxia.

A

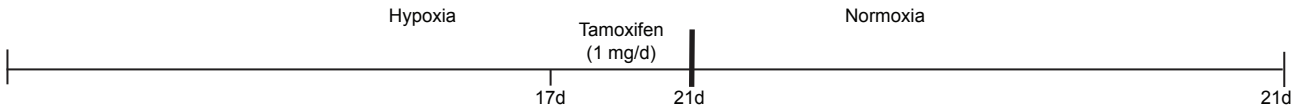

Acta2-CreER, Vhl$^{(flox/flox)}$

B

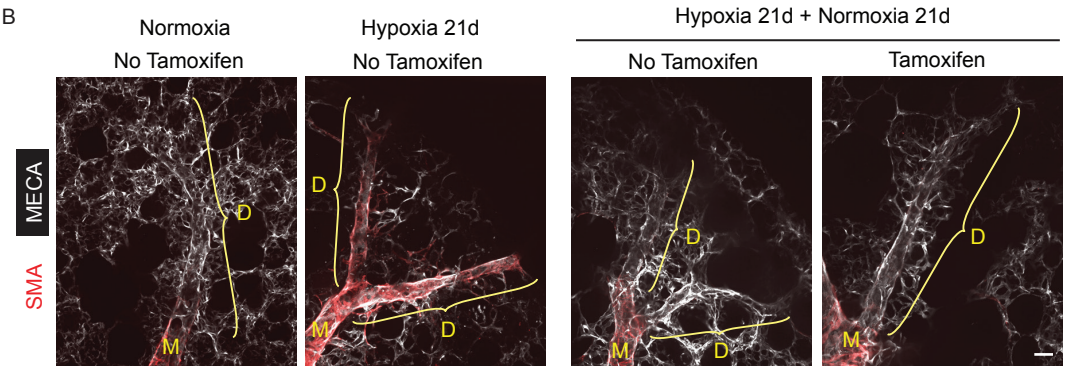

C

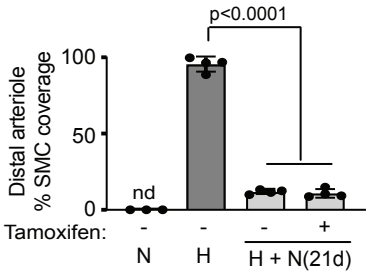

D

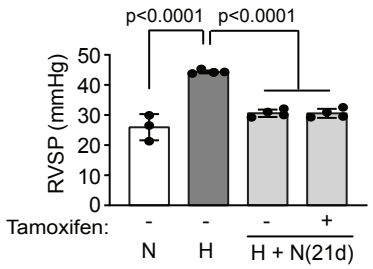

E

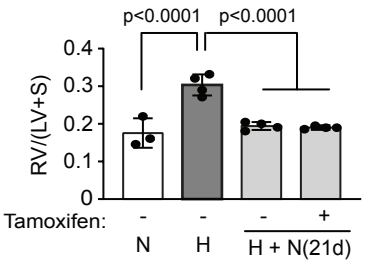

Cdh5-CreER, Vhl$^{(flox/flox)}$

F

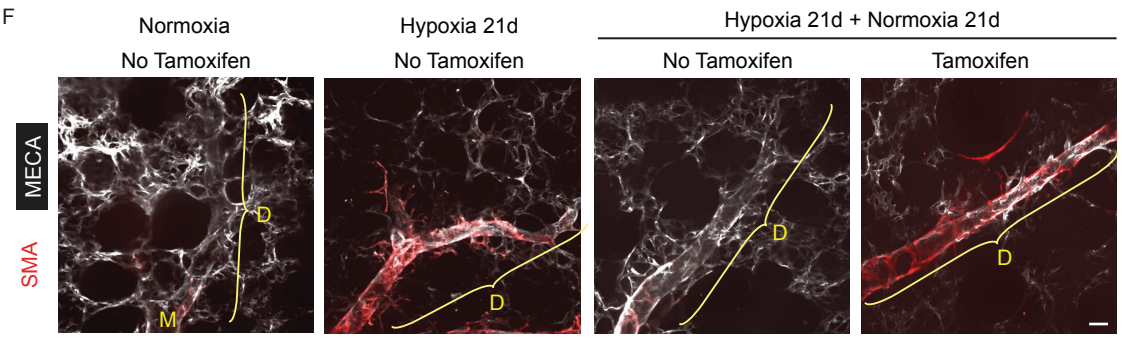

G

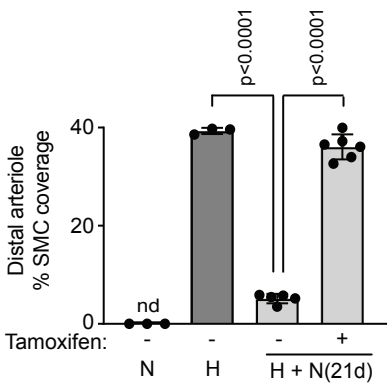

H

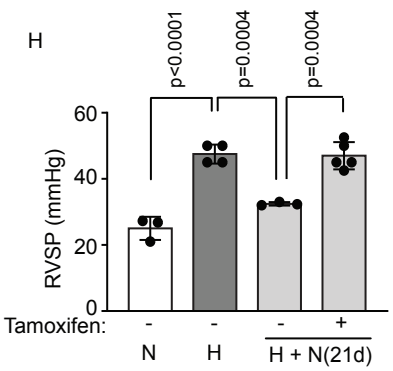

I

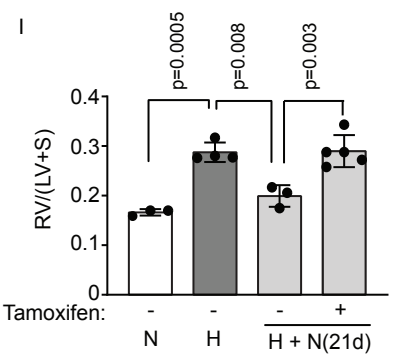

Figure 3. HIFα in ECs, but not in SMCs, is sufficient to retain distal pulmonary arteriole muscularization. A, Experimental strategy for (B-I). **B-I,** *Vhl*$^{(flox/flox)}$ mice also carrying *Acta-CreER*^{T2} (B-E) or *Cdh5-CreER*^{T2} (F-I) were exposed to hypoxia for 21 days and between hypoxia days 17-21, tamoxifen (1 mg/day) was or was not injected. Mice were analyzed at this time point or after 21 days of re-normoxia. In (B, F), lung vibratome sections were stained for SMA and MECA-32. M and D, middle and distal arterioles are denoted, respectively. In (C-E, and G-I), percentage of SMC coverage of distal arterioles, RVSP and RV weight ratio were measured as indicated. n=3-5 mice (2 males, 1-3 females) per experimental group; multi-factor ANOVA with Tukey's multiple comparison test. N, normoxia; H, hypoxia; H+N, hypoxia followed by normoxia. nd, not detected. Scale bars, 20 μm.

A

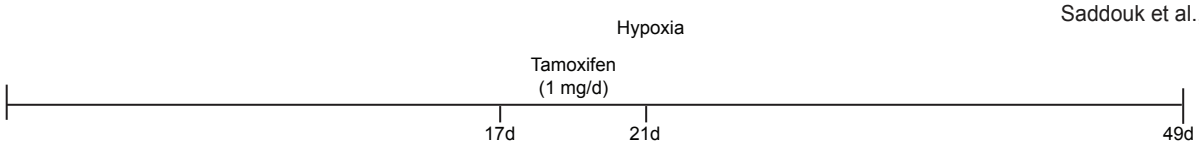

Cdh5-CreER, Hif1a$^{(flox/flox)}$

B

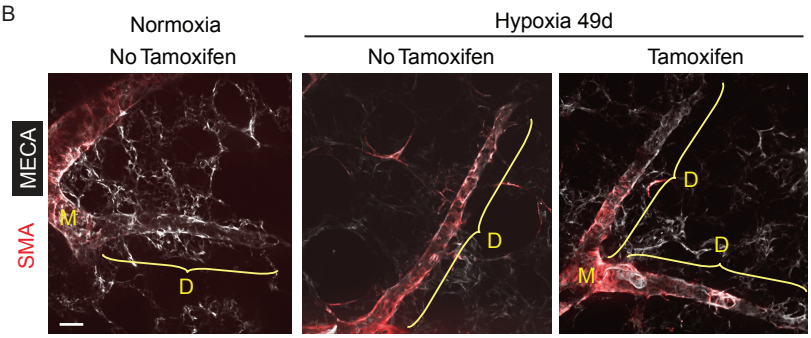

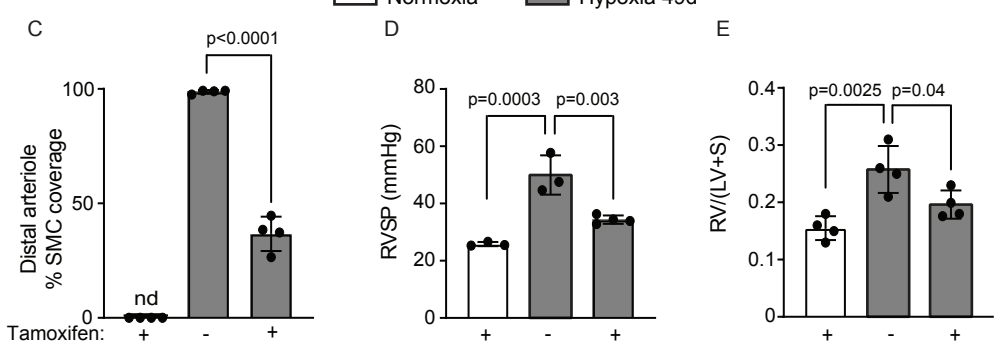

Cdh5-CreER, Hif2a$^{(flox/flox)}$

F

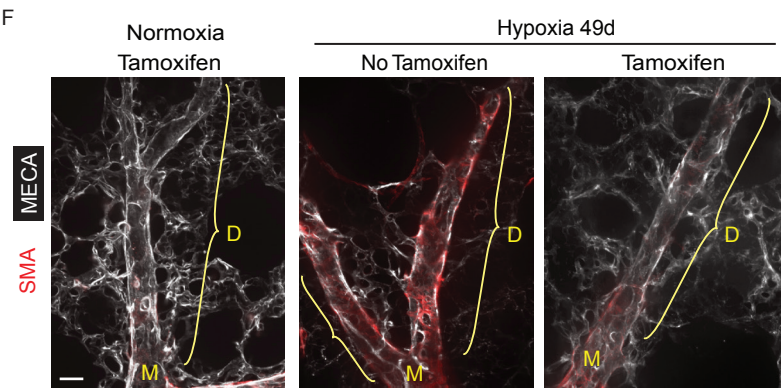

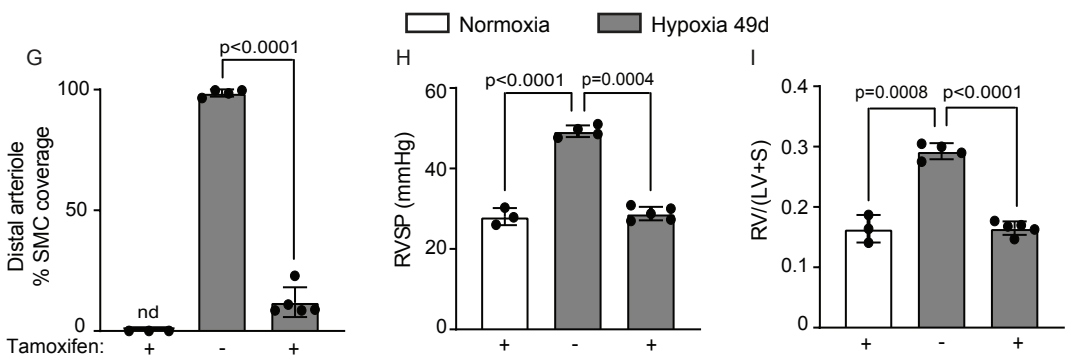

Figure 4. EC deletion of *Hif1a* or *Hif2a* attenuates established distal arteriole muscularization and PH. A. Experimental strategy for (B-I). **B-I,** *Cdh5-CreER*^{T2} mice carrying *Hif1a*$^{(flox/flox)}$ (B-E) or *Hif2a*$^{(flox/flox)}$ (F-I) were exposed to hypoxia for 49 days and tamoxifen (1 mg/day) was or was not administered between hypoxia days 17-21. In (B, F), vibratome lung sections were stained for SMA and MECA-32. In (C-E and G-I), percentage of SMC coverage of distal arterioles, RVSP and RV weight ratio were measured as indicated. n=3-5 mice (2 males, 1-3 females) per experimental group and 3 arterioles per mouse; multi-factor ANOVA with Tukey's multiple comparison test. nd, not detected. Scale bars, 20 µm.

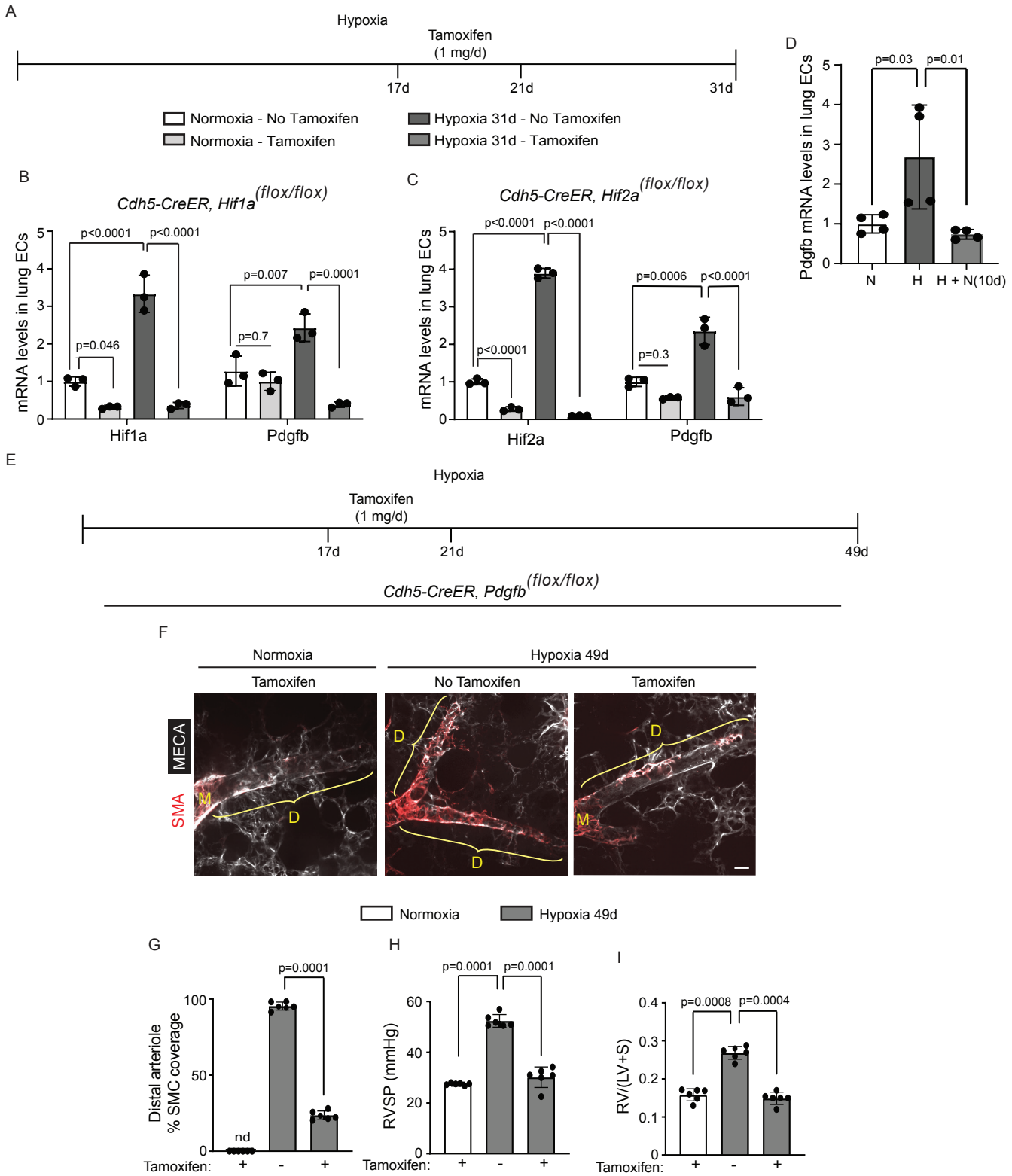
A
Hypoxia
Tamoxifen
(1 mg/d)
17d
21d
31d
Normoxia - No Tamoxifen
Normoxia - Tamoxifen
Hypoxia 31d - No Tamoxifen
Hypoxia 31d - Tamoxifen
B
Cdh5-CreER, Hif1a(flox/flox)
mRNA levels in lung ECs
p<0.0001
p<0.0001
p=0.046
p=0.007
p=0.0001
p=0.7
Hif1a
Pdgfb
C
Cdh5-CreER, Hif2a(flox/flox)
mRNA levels in lung ECs
p<0.0001
p<0.0001
p<0.0001
p=0.0006
p<0.0001
p=0.3
Hif2a
Pdgfb
D
Pdgfb mRNA levels in lung ECs
p=0.03
p=0.01
N
H
H + N(10d)
E
Hypoxia
Tamoxifen
(1 mg/d)
17d
21d
49d
Cdh5-CreER, Pdgfb(flox/flox)
F
Normoxia
Hypoxia 49d
Tamoxifen
No Tamoxifen
Tamoxifen
MECA
SMA
M
D
D
D
D
M
Normoxia
Hypoxia 49d
G
Distal arteriole
% SMC coverage
p=0.0001
nd
Tamoxifen:
+
-
+
H
RVSP (mmHg)
p=0.0001
p=0.0001
Tamoxifen:
+
-
+
I
RV/(LV+S)
p=0.0008
p=0.0004
Tamoxifen:
+
-
+

Figure 5. Deletion of EC *Pdgfb* attenuates established distal arteriole muscularization and PH. A, Experimental strategy for (B, C). **B, C,** *Cdh5-CreER*^{T2} mice carrying *Hif1a*$^{(flox/flox)}$ or *Hif2a*$^{(flox/flox)}$ were treated with hypoxia for 31 days and tamoxifen (1 mg/day) was or was not administered between hypoxia days 17-21. At 31 days, ECs were isolated by FACS, and Hif1a, Hif2a and Pdgfb transcript levels were measured by qRT-PCR. n=3 mice (2 males, 1 female) per experimental group. **D,** Wild type mice were exposed to normoxia (N) or hypoxia (H) for 21 days followed by normoxia for 10 days, and ECs were isolated by FACS. *Pdgfb* transcript levels were measured with qRT-PCR. n=4 mice (2 males, 2 females) per experimental group. **E,** Experimental strategy for (F-I). **F,** *Cdh5-CreER*^{T2}*, Pdgfb*$^{(flox/flox)}$ mice were exposed to hypoxia for 49 days, and tamoxifen (1 mg/day) was or was not administered between hypoxia days 17-21. Vibratome lung sections were stained for SMA and MECA-32. **G-I**, Percentage of distal arterioles covered by SMCs, RVSP and RV weight ratio were measured, respectively. n=6 mice (3 males, 3 females) per experimental group and 3 arterioles per mouse. nd, not detected. Multi-factor ANOVA with Tukey's multiple comparison test was used (B-D, G-I). Scale bar, 20 µm.

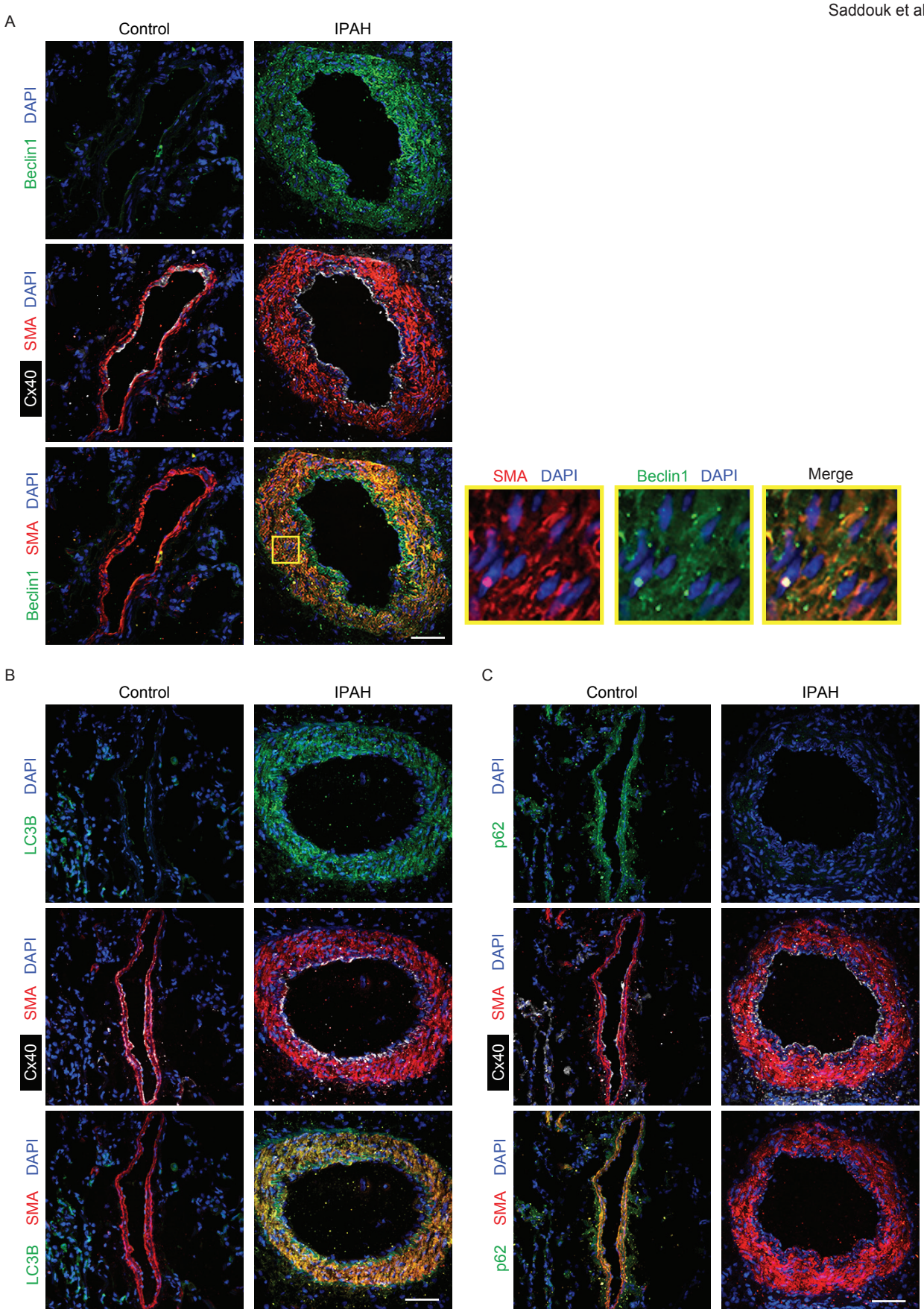
A
Control
IPAH
DAPI
Beclin1
DAPI
SMA
Cx40
DAPI
SMA
Beclin1
SMA DAPI
Beclin1 DAPI
Merge
B
Control
IPAH
DAPI
LC3B
DAPI
SMA
Cx40
DAPI
SMA
LC3B
C
Control
IPAH
DAPI
p62
DAPI
SMA
Cx40
DAPI
SMA
p62

Figure 6. In human IPAH, autophagy is upregulated in pulmonary arteriole SMCs. Immunohistochemical staining for Beclin1, LC3B, and p62 as markers of autophagy in combination with SMA, Cx40 and DAPI in lungs of human control and IPAH patients (n=4). Close-up of boxed region in (A) is shown to the right. Scale bars, 50 µm.

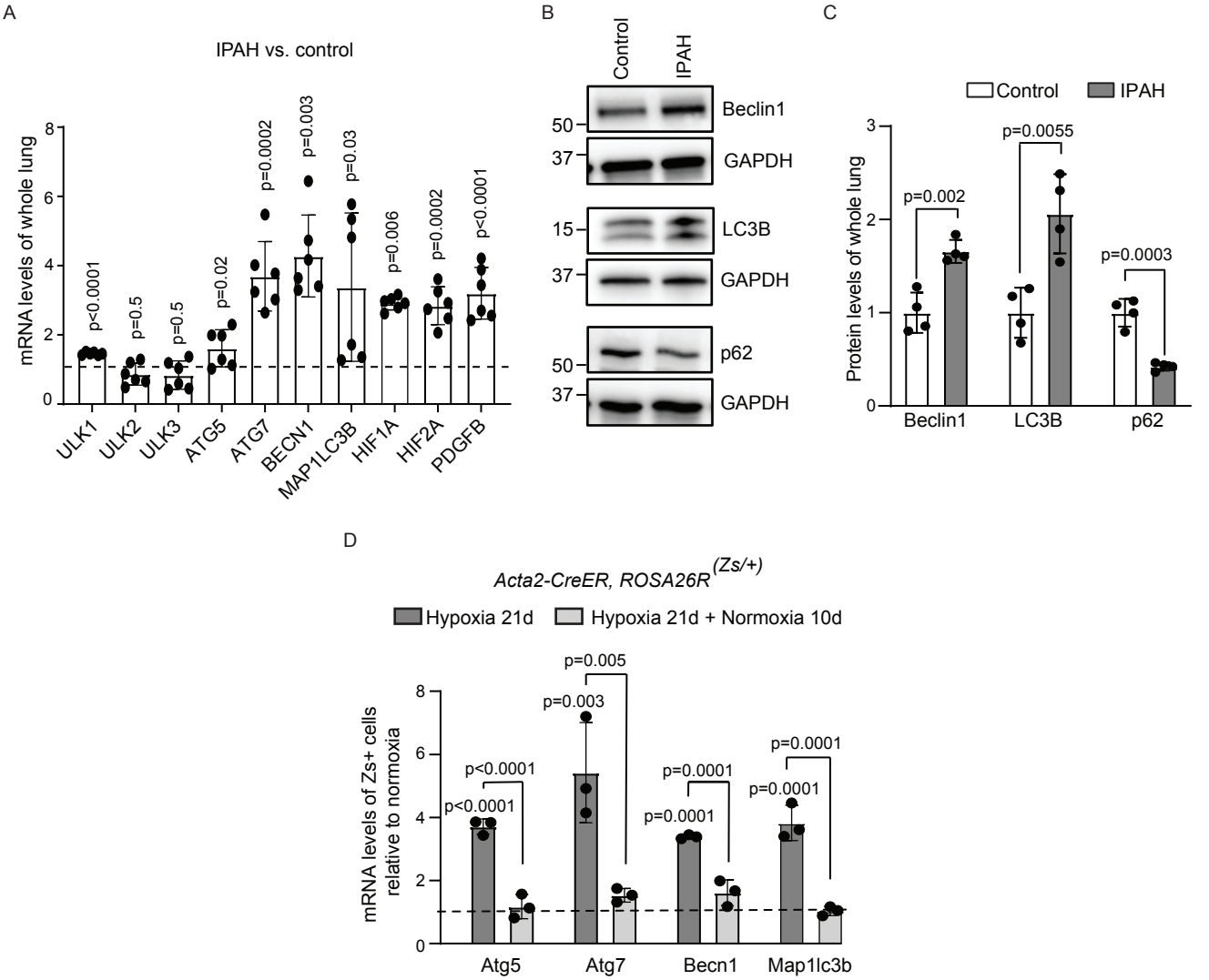
A
IPAH vs. control
mRNA levels of whole lung
p<0.0001
p=0.5
p=0.5
p=0.02
p=0.0002
p=0.003
p=0.03
p=0.006
p=0.0002
p<0.0001
ULK1
ULK2
ULK3
ATG5
ATG7
BECN1
MAP1LC3B
HIF1A
HIF2A
PDGFB
B
Control
IPAH
Beclin1
GAPDH
LC3B
GAPDH
p62
GAPDH
50
37
15
37
50
37
C
Control
IPAH
Protein levels of whole lung
p=0.002
p=0.0055
p=0.0003
Beclin1
LC3B
p62
D
Acta2-CreER, ROSA26R(Zs/+)
Hypoxia 21d
Hypoxia 21d + Normoxia 10d
mRNA levels of Zs+ cells relative to normoxia
p<0.0001
p<0.0001
p=0.003
p=0.005
p=0.0001
p=0.0001
p=0.0001
p=0.0001
Atg5
Atg7
Becn1
Map1lc3b

Figure 7. Autophagy-related genes are upregulated in lungs of IPAH humans and lung SMCs of hypoxic mice and downregulated in murine lung SMCs with re-normoxia. A, qRT-PCR analysis of autophagy-related gene products and HIF1A, HIF2A and PDGFB from lung lysates of patients with IPAH compared with that of control humans (n=6). **B,** Western blots of lung lysates of IPAH patients and controls probed for Beclin1, LC3B, p62 and GAPDH. **C,** Densitometry of protein bands shown in (B) relative to GAPDH and normalized to control (n=4). **D,** *Acta2-CreER*^{T2}*, ROSA26R*$^{(Zs/+)}$ mice were induced with tamoxifen, rested for 5 days, exposed to normoxia or hypoxia for 21 days or to hypoxia for 21 days followed by re-normoxia for 10 days. Lung Zs^{+} cells were isolated by FACS, and the expression of autophagy genes Atg5, Atg7, Becn1 and Map1lc3b was analyzed by qRT-PCR and normalized to normoxia. n=3 mice (1 male, 2 females) per experimental group. Student's *t*-test (A, C) or multi-factor ANOVA with Tukey's multiple comparison test (D) was used.

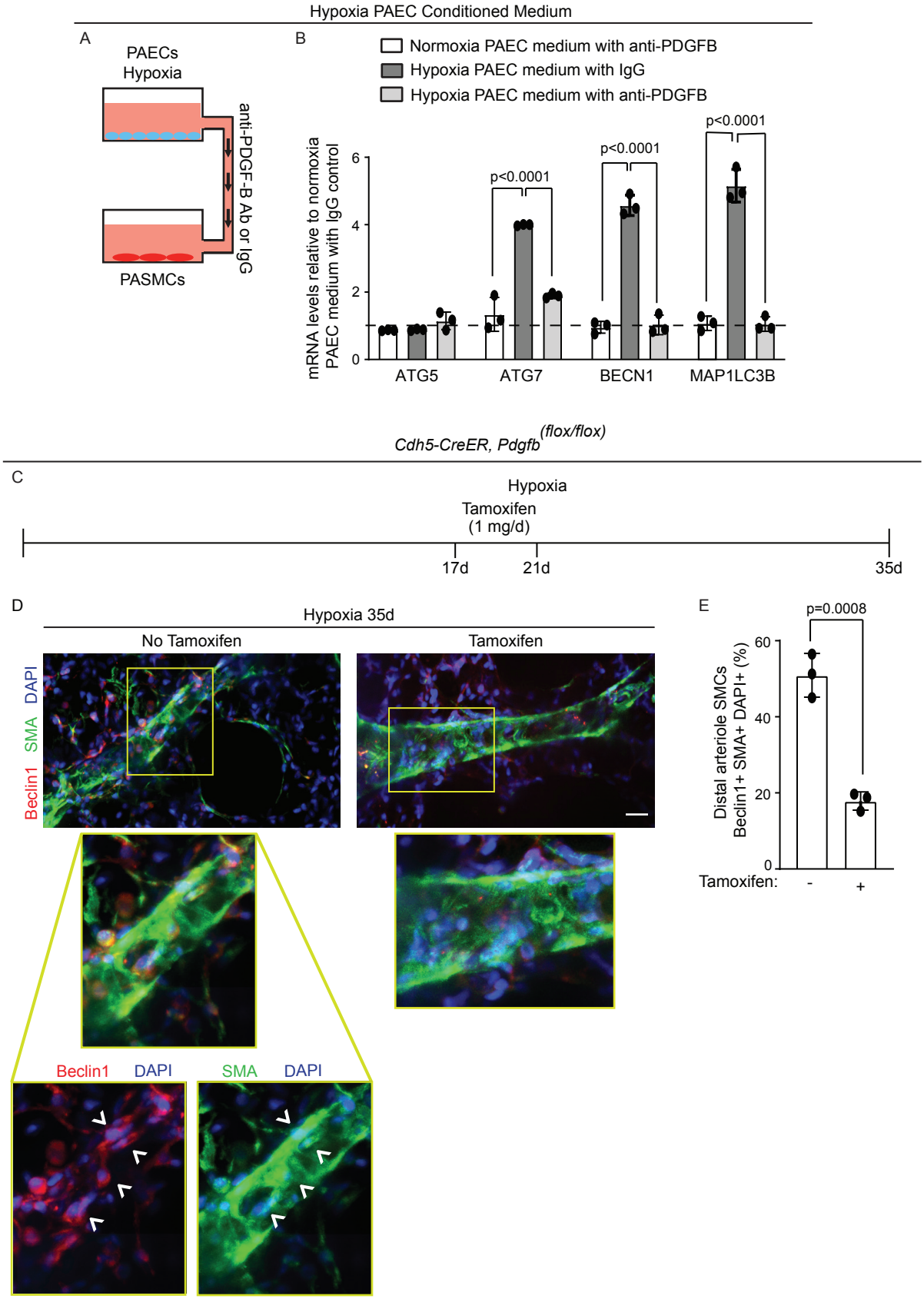
Hypoxia PAEC Conditioned Medium
A
PAECs
Hypoxia
anti-PDGF-B Ab or IgG
PASMCs
B
Normoxia PAEC medium with anti-PDGFB
Hypoxia PAEC medium with IgG
Hypoxia PAEC medium with anti-PDGFB
mRNA levels relative to normoxia PAEC medium with IgG control
p<0.0001
p<0.0001
p<0.0001
ATG5
ATG7
BECN1
MAP1LC3B
Cdh5-CreER, Pdgfb(flox/flox)
C
Hypoxia
Tamoxifen
(1 mg/d)
17d
21d
35d
D
Hypoxia 35d
No Tamoxifen
Tamoxifen
DAPI
SMA
Beclin1
Beclin1
DAPI
SMA
DAPI
E
p=0.0008
Distal arteriole SMCs
Beclin1+ SMA+ DAPI+ (%)
Tamoxifen:
-
+

Figure 8. Pharmacological or genetic inhibition of EC-derived PDGF-B in mice or in culture, respectively downregulates Beclin1 in SMCs. A, Experimental strategy for (B). **B,** Human PAECs were exposed to normoxia or hypoxia (3% O_2) for 16 h, and the conditioned medium was collected and pre-treated with either anti-PDGF-B blocking antibody or IgG isotype control for 1 h. Human PASMCs were incubated with the pre-treated PAEC medium in normoxic conditions for 48 h, and then qRT-PCR was used to assess mRNA levels of ATG5, ATG7, BECN1 and MAP1LC3B in the PASMCs. Transcript levels relative to 18S rRNA were normalized to normoxia PAECs medium treated with IgG (dashed line). n=3; multi-factor ANOVA with Tukey's multiple comparison test. **C,** Experimental strategy for (D, E). **D**, *Cdh5-CreER*^{T2}*, Pdgfb*$^{(flox/flox)}$ mice were exposed to hypoxia for 35 days and tamoxifen (1 mg/day) was or was not administered between hypoxia days 17-21. Vibratome lung sections were stained for Beclin1, SMA and nuclei (DAPI). Close-ups of boxed region are shown below. Arrowheads indicate Beclin1^{+}SMA^{+} cells. **E,** Quantification of the percent of distal arteriole SMCs that are Beclin1^{+}. n=3 mice (2 males, 1 female) per experimental group, 3-4 arterioles analyzed per mouse; Student's *t*-test. Scale bar, 20 µm.

Acta2-CreER, ROSA26R $^{(Zs/+)}$

A

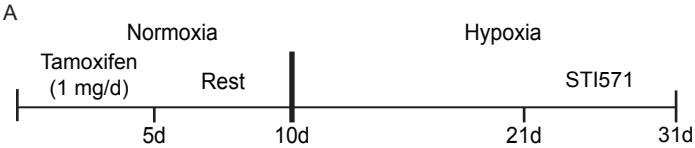

B

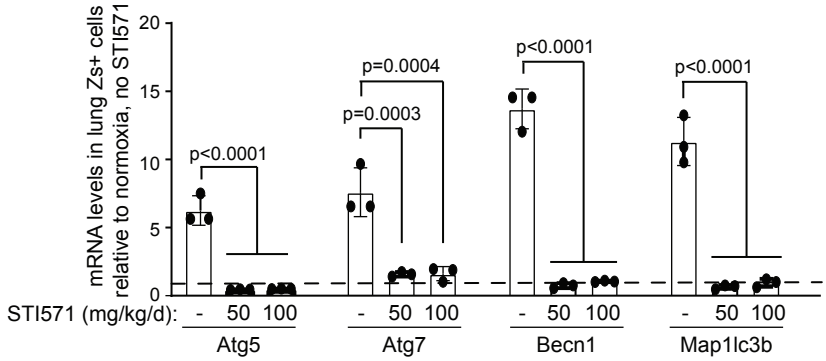

C

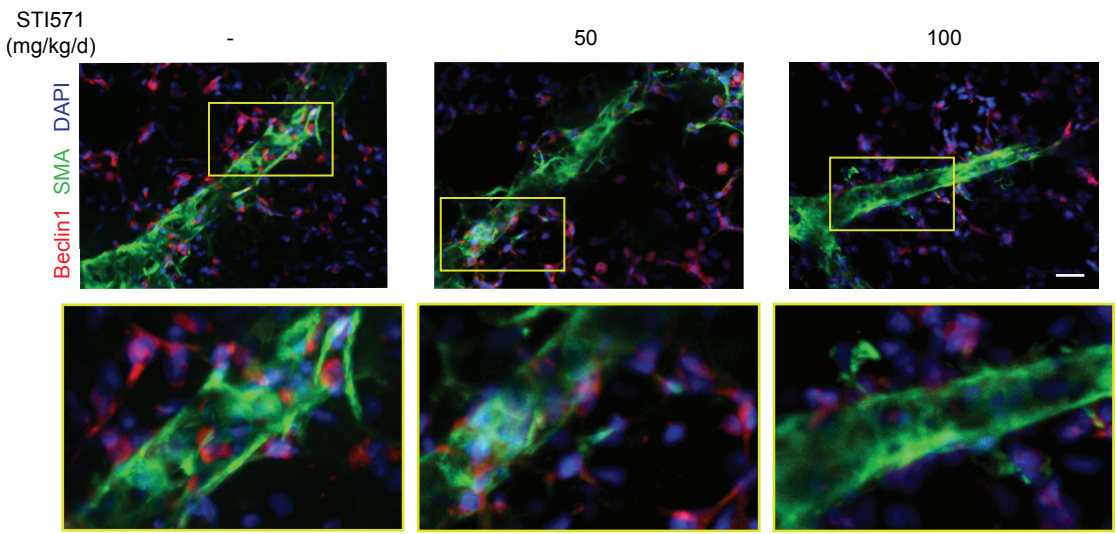

D

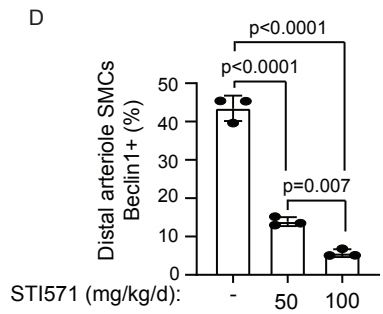

Figure 9. Inhibition of tyrosine receptor kinases, including PDGFRs, attenuates lung SMC Beclin1 levels. A, Experimental strategy for (B-D). **B,** *Acta2-CreER*^{T2}*, ROSA26R*$^{(Zs/+)}$ mice were exposed to hypoxia or normoxia for 31 days and STI571 was administered at 0, 50 or 100 mg/kg/d by daily intraperitoneal injections between hypoxia days 21-31. Lung Zs^{+} SMCs were isolated by FACS, and expression levels of Atg5, Atg7, Becn1 and Map1lc3b with hypoxia relative to normoxia, no STI571 were analyzed by qRT-PCR. n=3 mice (2 males, 1 female) per experimental group. **C**, Vibratome lung sections were stained for Beclin1, SMA and nuclei (DAPI). Close-ups of boxed regions are shown below. **D,** Quantification of the percent of distal arteriole SMCs that are Belclin1^{+}. n=3 mice (1 male, 2 female) per experimental group, 3-4 arterioles analyzed per mouse. Multi-factor ANOVA with Tukey's multiple comparison test was used (B, D). Scale bar, 20 µm.

Acta2-CreER, Becn1 (flox/flox)

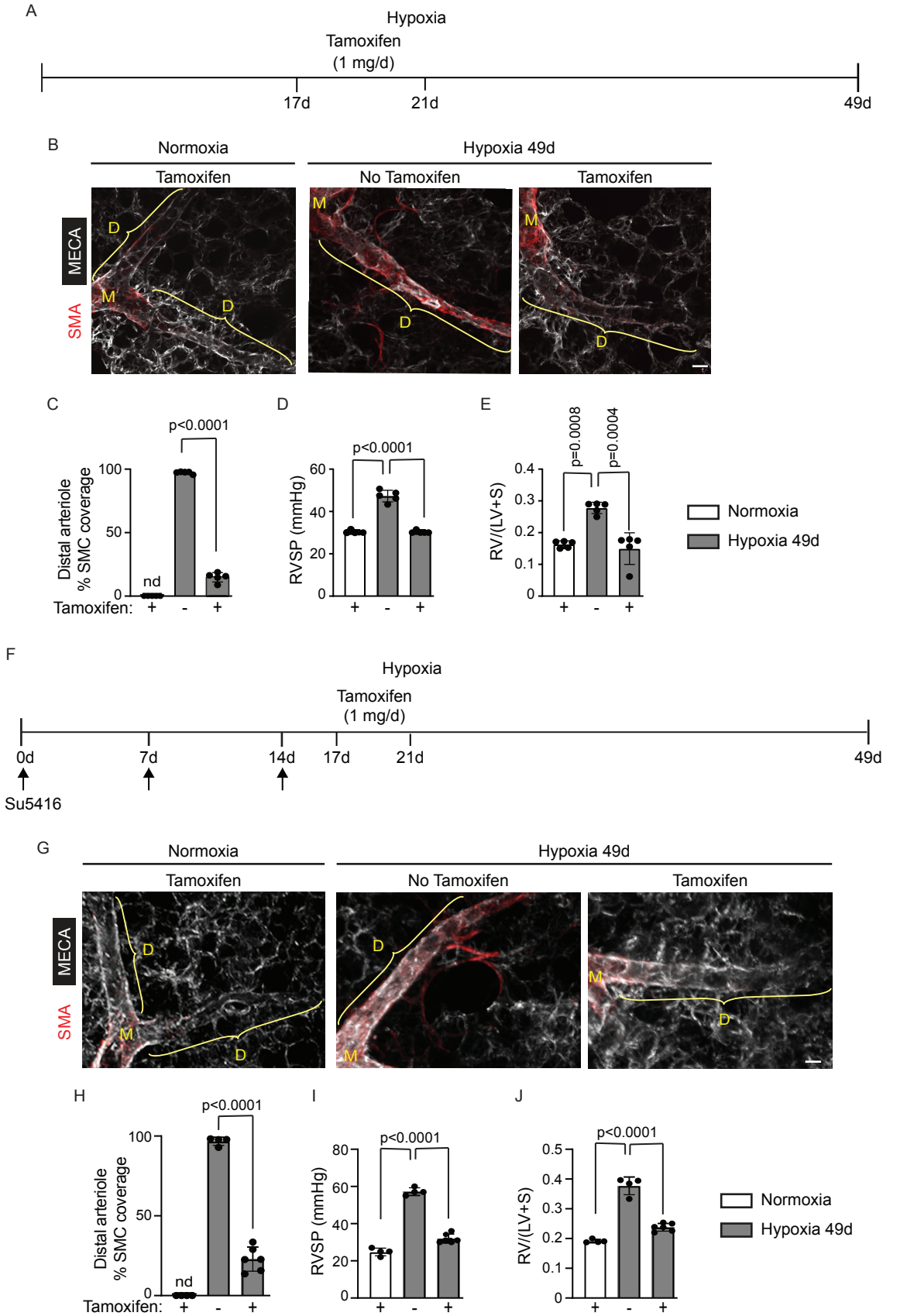

Figure 10. SMC deletion of *Becn1* attenuates established distal arteriole muscularization and PH. A, Experimental strategy for (B-E). **B,** *Acta2-CreER^{T2}, Becn1$^{(flox/flox)}$* mice were exposed to hypoxia for 49 days and tamoxifen (1 mg/day) was or was not administered between hypoxia days 17-21. Vibratome lung sections were stained for SMA and MECA-32. **C-E,** Percentage of SMC coverage of distal arterioles, RVSP and RV weight ratio were measured, respectively. n=5 mice (3 males, 2 females) per experimental group, 3 arterioles per mouse; multi-factor ANOVA with Tukey's multiple comparison test. **F,** Experimental strategy for (G-J). **G,** *Acta2-CreER^{T2}, Becn1$^{(flox/flox)}$* mice were exposed to hypoxia for 49 days. Sugen 5416 was administered at days 0, 7 and 14 by subcutaneous injection (20 mg/kg/dose), and tamoxifen (1 mg/day) was or was not administered between hypoxia days 17-21. Vibratome lung sections were stained for SMA and MECA-32. **H-J,** Percentage of SMC coverage of distal arterioles, RVSP and RV weight ratio were measured, respectively. n=4-6 mice (2 males, 2-4 females) per experimental group, 3 arterioles per mouse; multi-factor ANOVA with Tukey's multiple comparison test. Scale bars, 20 µm.

Acta2-CreER, ROSA26R $^{(Zs/+)}$

A

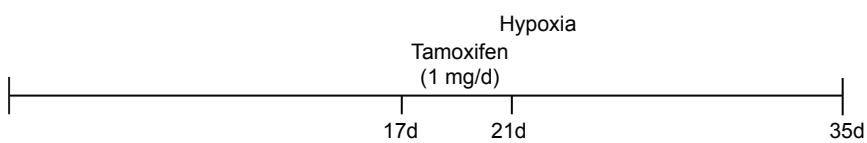

B

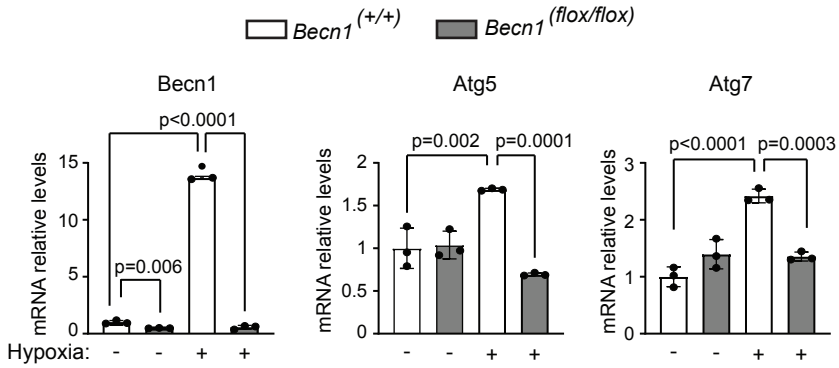

Figure 11. *Becn1* deletion in SMCs attenuates hypoxia-induced increase in Atg5 and Atg7. **A,** Experimental strategy for (B). **B,** *Acta2-CreER*^{T2}, *ROSA26R*$^{(Zs/+)}$ mice also carrying *Becn1*$^{(flox/flox)}$ or *Becn1*$^{(+/+)}$ were exposed to hypoxia for 35 days, and tamoxifen (1 mg/day) was administered between days 17-21. Zs^{+} cells were isolated by FACS, and mRNA levels of Becn1, Atg5 and Atg7 were measured by qRT-PCR and normalized to *Becn1*$^{(+/+)}$, normoxia. n=3 mice (2 males, 1 female) per experimental group; multi-factor ANOVA with Tukey's multiple comparison test. nd, not detected.

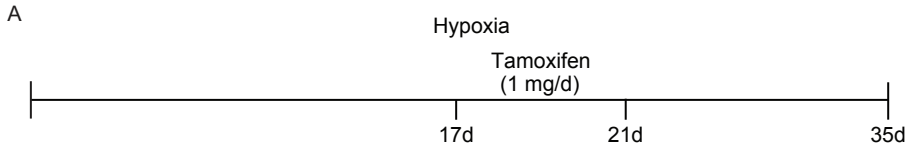
A
Hypoxia
Tamoxifen
(1 mg/d)
17d
21d
35d

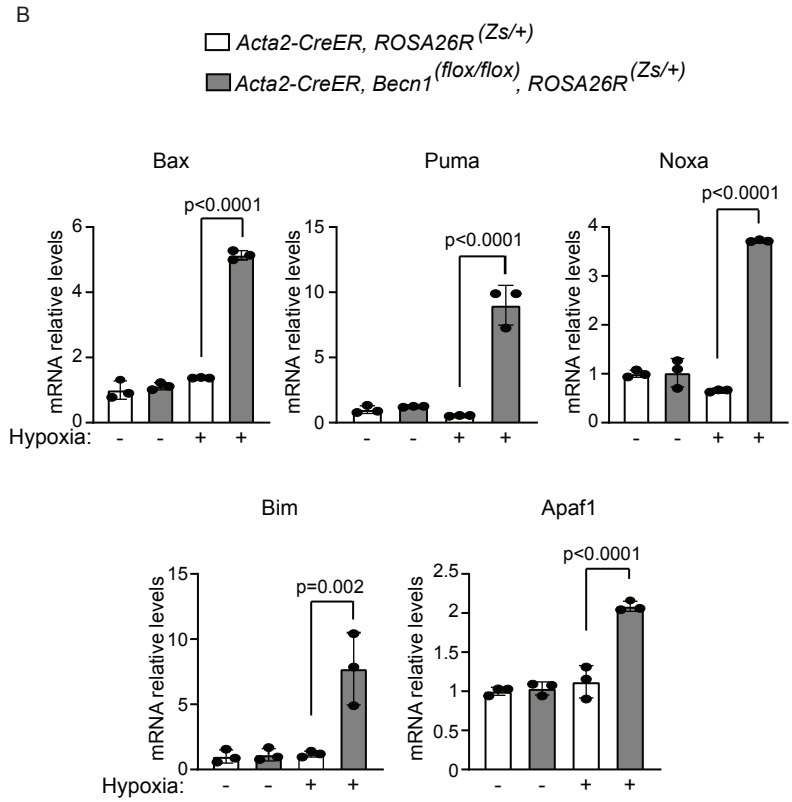
B
Acta2-CreER, ROSA26R (Zs/+)
Acta2-CreER, Becn1 (flox/flox), ROSA26R (Zs/+)
Bax
Puma
Noxa
Bim
Apaf1
mRNA relative levels
p<0.0001
p<0.0001
p<0.0001
p=0.002
p<0.0001
Hypoxia: - - + +

Figure 12. Pro-apoptosis markers are upregulated by SMC deletion of *Becn1*. A, Experimental strategy for (B). **B,** *Acta2-CreER*^{T2}*, ROSA26R*$^{(Zs/+)}$ mice carrying *Becn1*$^{(flox/flox)}$ or *Becn1*$^{(+/+)}$ were exposed to hypoxia for 35 days and tamoxifen (1 mg/day) was administered between hypoxia days 17-21. Zs^+ cells were isolated by FACS, and the mRNA levels of pro-apoptosis markers were measured by qRT-PCR. N=3 mice (2 males, 1 female) per experimental group; multi-factor ANOVA with Tukey's multiple comparison test.

Acta2-CreER, Becn1$^{(flox/flox)}$

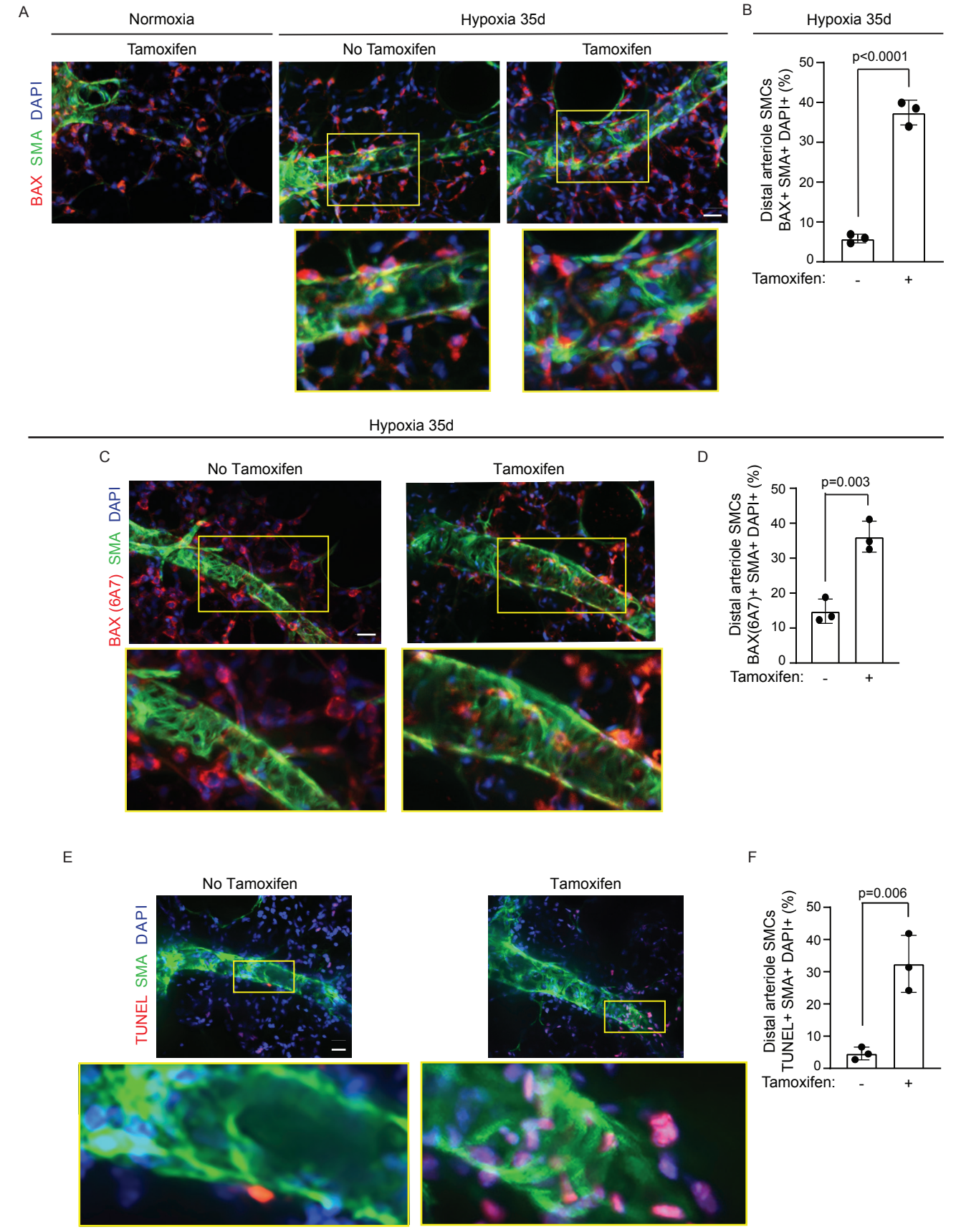

Figure 13. Deletion of *Becn1* in SMCs induces apoptosis of distal arteriole SMCs. A-F, *Acta2-CreER*^{T2}*, Becn1*$^{(flox/flox)}$ mice were exposed to hypoxia for 35 days [or to normoxia in (A, left panel)] and tamoxifen (1 mg/day) was or was not administered between hypoxia days 17-21. Vibratome lung sections were stained for SMA, nuclei (DAPI) and either BAX (A), activated BAX (6A7) (C) or TUNEL (E). Close-ups of boxed regions are shown below. The percent of distal arteriole SMCs expressing BAX (B) activated BAX (D) or TUNEL (F) was quantified. n=3 mice (2 males, 1 female) per experimental group, 3-4 arteriole analyzed per mouse; Student's *t*-test. Scale bars, 20 µm.

References

1. Mahapatra S, Nishimura RA, Sorajja P, Cha S, and McGoon MD. Relationship of pulmonary arterial capacitance and mortality in idiopathic pulmonary arterial hypertension. *J Am Coll Cardiol.* 2006;47(4):799-803.
2. Benza RL, Miller DP, Barst RJ, Badesch DB, Frost AE, and McGoon MD. An evaluation of long-term survival from time of diagnosis in pulmonary arterial hypertension from the REVEAL Registry. *Chest.* 2012;142(2):448-56.
3. Arias-Stella J, Kruger H, and Recavarren S. Pathology of chronic mountain sickness. *Thorax.* 1973;28(6):701-8.
4. Arias-Stella J, and Saldana M. The Terminal Portion of the Pulmonary Arterial Tree in People Native to High Altitudes. *Circulation.* 1963;28:915-25.
5. Sime F, Penaloza D, and Ruiz L. Bradycardia, increased cardiac output, and reversal of pulmonary hypertension in altitude natives living at sea level. *Br Heart J.* 1971;33(5):647-57.
6. Xu XQ, and Jing ZC. High-altitude pulmonary hypertension. *Eur Respir Rev.* 2009;18(111):13-7.
7. Sluiter I, van Heijst A, Haasdijk R, Kempen MB, Boerema-de Munck A, Reiss I, et al. Reversal of pulmonary vascular remodeling in pulmonary hypertensive rats. *Exp Mol Pathol.* 2012;93(1):66-73.
8. Chen J, Wang YX, Dong MQ, Zhang B, Luo Y, Niu W, et al. Reoxygenation Reverses Hypoxic Pulmonary Arterial Remodeling by Inducing Smooth Muscle Cell Apoptosis via Reactive Oxygen Species-Mediated Mitochondrial Dysfunction. *J Am Heart Assoc.* 2017;6(6).
9. Semenza GL. Hypoxia-inducible factors in physiology and medicine. *Cell.* 2012;148(3):399-408.
10. Sheikh AQ, Saddouk FZ, Ntokou A, Mazurek R, and Greif DM. Cell Autonomous and Non-cell Autonomous Regulation of SMC Progenitors in Pulmonary Hypertension. *Cell Rep.* 2018;23(4):1152-65.
11. Waypa GB, and Schumacker PT. Roles of HIF1 and HIF2 in pulmonary hypertension: it all depends on the context. *Eur Respir J.* 2019;54(6).
12. Yu AY, Shimoda LA, Iyer NV, Huso DL, Sun X, McWilliams R, et al. Impaired physiological responses to chronic hypoxia in mice partially deficient for hypoxia-inducible factor 1alpha. *J Clin Invest.* 1999;103(5):691-6.
13. Brusselmans K, Compernolle V, Tjwa M, Wiesener MS, Maxwell PH, Collen D, et al. Heterozygous deficiency of hypoxia-inducible factor-2alpha protects mice against pulmonary hypertension and right ventricular dysfunction during prolonged hypoxia. *J Clin Invest.* 2003;111(10):1519-27.
14. Ball MK, Waypa GB, Mungai PT, Nielsen JM, Czech L, Dudley VJ, et al. Regulation of hypoxia-induced pulmonary hypertension by vascular smooth muscle hypoxia-inducible factor-1alpha. *Am J Respir Crit Care Med.* 2014;189(3):314-24.
15. Cowburn AS, Crosby A, Macias D, Branco C, Colaco RD, Southwood M, et al. HIF2alpha-arginase axis is essential for the development of pulmonary hypertension. *Proc Natl Acad Sci U S A.* 2016;113(31):8801-6.

16. Kapitsinou PP, Rajendran G, Astleford L, Michael M, Schonfeld MP, Fields T, et al. The Endothelial Prolyl-4-Hydroxylase Domain 2/Hypoxia-Inducible Factor 2 Axis Regulates Pulmonary Artery Pressure in Mice. *Mol Cell Biol.* 2016;36(10):1584-94.
17. Dahal BK, Heuchel R, Pullamsetti SS, Wilhelm J, Ghofrani HA, Weissmann N, et al. Hypoxic pulmonary hypertension in mice with constitutively active platelet-derived growth factor receptor-beta. *Pulm Circ.* 2011;1(2):259-68.
18. Izikki M, Guignabert C, Fadel E, Humbert M, Tu L, Zadigue P, et al. Endothelial-derived FGF2 contributes to the progression of pulmonary hypertension in humans and rodents. *J Clin Invest.* 2009;119(3):512-23.
19. Savale L, Tu L, Rideau D, Izziki M, Maitre B, Adnot S, et al. Impact of interleukin-6 on hypoxia-induced pulmonary hypertension and lung inflammation in mice. *Respir Res.* 2009;10:6.
20. Wang Z, Li AY, Guo QH, Zhang JP, An Q, Guo YJ, et al. Effects of cyclic intermittent hypoxia on ET-1 responsiveness and endothelial dysfunction of pulmonary arteries in rats. *PLoS One.* 2013;8(3):e58078.
21. Wu YC, Wang WT, Lee SS, Kuo YR, Wang YC, Yen SJ, et al. Glucagon-Like Peptide-1 Receptor Agonist Attenuates Autophagy to Ameliorate Pulmonary Arterial Hypertension through Drp1/NOX- and Atg-5/Atg-7/Beclin-1/LC3β Pathways. *Int J Mol Sci.* 2019;20(14).
22. Salabei JK, Cummins TD, Singh M, Jones SP, Bhatnagar A, and Hill BG. PDGF-mediated autophagy regulates vascular smooth muscle cell phenotype and resistance to oxidative stress. *Biochem J.* 2013;451(3):375-88.
23. Mao M, Yu X, Ge X, Gu R, Li Q, Song S, et al. Acetylated cyclophilin A is a major mediator in hypoxia-induced autophagy and pulmonary vascular angiogenesis. *J Hypertens.* 2017;35(4):798-809.
24. Liu Y, Xu Y, Zhu J, Li H, Zhang J, Yang G, et al. Metformin Prevents Progression of Experimental Pulmonary Hypertension via Inhibition of Autophagy and Activation of Adenosine Monophosphate-Activated Protein Kinase. *J Vasc Res.* 2019;56(3):117-28.
25. Lee SJ, Kim HP, Jin Y, Choi AM, and Ryter SW. Beclin 1 deficiency is associated with increased hypoxia-induced angiogenesis. *Autophagy.* 2011;7(8):829-39.
26. Shimoda LA, and Laurie SS. Vascular remodeling in pulmonary hypertension. *J Mol Med (Berl).* 2013;91(3):297-309.
27. Sheikh AQ, Lighthouse JK, and Greif DM. Recapitulation of developing artery muscularization in pulmonary hypertension. *Cell Rep.* 2014;6(5):809-17.
28. Sheikh AQ, Misra A, Rosas IO, Adams RH, and Greif DM. Smooth muscle cell progenitors are primed to muscularize in pulmonary hypertension. *Sci Transl Med.* 2015;7(308):308ra159.
29. Ntokou A, Dave JM, Kauffman AC, Sauler M, Ryu C, Hwa J, et al. Macrophage-derived PDGF-B induces muscularization in murine and human pulmonary hypertension. *JCI Insight.* 2021;6(6).
30. Kretschmer S, Dethlefsen I, Hagner-Benes S, Marsh LM, Garn H, and König P. Visualization of Intrapulmonary Lymph Vessels in Healthy and Inflamed Murine Lung Using CD90/Thy-1 as a Marker. *PLOS ONE.* 2013;8(2):e55201.
31. Ehling M, Adams S, Benedito R, and Adams RH. Notch controls retinal blood vessel maturation and quiescence. *Development.* 2013;140(14):3051-61.

32. Labrousse-Arias D, Castillo-Gonzalez R, Rogers NM, Torres-Capelli M, Barreira B, Aragones J, et al. HIF-2alpha-mediated induction of pulmonary thrombospondin-1 contributes to hypoxia-driven vascular remodelling and vasoconstriction. *Cardiovasc Res.* 2016;109(1):115-30.
33. Dai Z, Li M, Wharton J, Zhu MM, and Zhao YY. Prolyl-4 Hydroxylase 2 (PHD2) Deficiency in Endothelial Cells and Hematopoietic Cells Induces Obliterative Vascular Remodeling and Severe Pulmonary Arterial Hypertension in Mice and Humans Through Hypoxia-Inducible Factor-2alpha. *Circulation.* 2016;133(24):2447-58.
34. Epstein AC, Gleadle JM, McNeill LA, Hewitson KS, O'Rourke J, Mole DR, et al. C. elegans EGL-9 and mammalian homologs define a family of dioxygenases that regulate HIF by prolyl hydroxylation. *Cell.* 2001;107(1):43-54.
35. Ivan M, Kondo K, Yang H, Kim W, Valiando J, Ohh M, et al. HIFalpha targeted for VHL-mediated destruction by proline hydroxylation: implications for O2 sensing. *Science.* 2001;292(5516):464-8.
36. Long L, Yang X, Southwood M, Lu J, Marciniak SJ, Dunmore BJ, et al. Chloroquine prevents progression of experimental pulmonary hypertension via inhibition of autophagy and lysosomal bone morphogenetic protein type II receptor degradation. *Circ Res.* 2013;112(8):1159-70.
37. Lee SJ, Smith A, Guo L, Alastalo TP, Li M, Sawada H, et al. Autophagic protein LC3B confers resistance against hypoxia-induced pulmonary hypertension. *Am J Respir Crit Care Med.* 2011;183(5):649-58.
38. Schermuly RT, Dony E, Ghofrani HA, Pullamsetti S, Savai R, Roth M, et al. Reversal of experimental pulmonary hypertension by PDGF inhibition. *J Clin Invest.* 2005;115(10):2811-21.
39. Vitali SH, Hansmann G, Rose C, Fernandez-Gonzalez A, Scheid A, Mitsialis SA, et al. The Sugen 5416/hypoxia mouse model of pulmonary hypertension revisited: long-term follow-up. *Pulm Circ.* 2014;4(4):619-29.
40. Luo S, Garcia-Arencibia M, Zhao R, Puri C, Toh Pearl PC, Sadiq O, et al. Bim Inhibits Autophagy by Recruiting Beclin 1 to Microtubules. *Molecular Cell.* 2012;47(3):359-70.
41. McKnight NC, Zhong Y, Wold MS, Gong S, Phillips GR, Dou Z, et al. Beclin 1 is required for neuron viability and regulates endosome pathways via the UVRAG-VPS34 complex. *PLoS Genet.* 2014;10(10):e1004626.
42. Yue Z, Jin S, Yang C, Levine AJ, and Heintz N. Beclin 1, an autophagy gene essential for early embryonic development, is a haploinsufficient tumor suppressor. *Proc Natl Acad Sci U S A.* 2003;100(25):15077-82.
43. Dai Z, Zhu MM, Peng Y, Machireddy N, Evans CE, Machado R, et al. Therapeutic Targeting of Vascular Remodeling and Right Heart Failure in Pulmonary Arterial Hypertension with a HIF-2alpha Inhibitor. *Am J Respir Crit Care Med.* 2018;198(11):1423-34.
44. Hu CJ, Poth JM, Zhang H, Flockton A, Laux A, Kumar S, et al. Suppression of HIF2 signalling attenuates the initiation of hypoxia-induced pulmonary hypertension. *Eur Respir J.* 2019;54(6).
45. Abud EM, Maylor J, Undem C, Punjabi A, Zaiman AL, Myers AC, et al. Digoxin inhibits development of hypoxic pulmonary hypertension in mice. *Proc Natl Acad Sci U S A.* 2012;109(4):1239-44.

46. Kim YM, Barnes EA, Alvira CM, Ying L, Reddy S, and Cornfield DN. Hypoxia-inducible factor-1alpha in pulmonary artery smooth muscle cells lowers vascular tone by decreasing myosin light chain phosphorylation. *Circ Res.* 2013;112(9):1230-3.
47. Tang H, Babicheva A, McDermott KM, Gu Y, Ayon RJ, Song S, et al. Endothelial HIF-2alpha contributes to severe pulmonary hypertension due to endothelial-to-mesenchymal transition. *Am J Physiol Lung Cell Mol Physiol.* 2018;314(2):L256-L75.
48. Chandran RR, Xie Y, Gallardo-Vara E, Adams T, Garcia-Milian R, Kabir I, et al. Distinct roles of KLF4 in mesenchymal cell subtypes during lung fibrogenesis. *Nat Commun.* 2021;12(1):7179.
49. Hassoun PM, Mouthon L, Barbera JA, Eddahibi S, Flores SC, Grimminger F, et al. Inflammation, growth factors, and pulmonary vascular remodeling. *J Am Coll Cardiol.* 2009;54(1 Suppl):S10-S9.
50. ten Freyhaus H, Dumitrescu D, Berghausen E, Vantler M, Caglayan E, and Rosenkranz S. Imatinib mesylate for the treatment of pulmonary arterial hypertension. *Expert Opin Investig Drugs.* 2012;21(1):119-34.
51. Perros F, Montani D, Dorfmuller P, Durand-Gasselin I, Tcherakian C, Le Pavec J, et al. Platelet-derived growth factor expression and function in idiopathic pulmonary arterial hypertension. *Am J Respir Crit Care Med.* 2008;178(1):81-8.
52. Selimovic N, Bergh CH, Andersson B, Sakiniene E, Carlsten H, and Rundqvist B. Growth factors and interleukin-6 across the lung circulation in pulmonary hypertension. *Eur Respir J.* 2009;34(3):662-8.
53. Newman AAC, Serbulea V, Baylis RA, Shankman LS, Bradley X, Alencar GF, et al. Multiple cell types contribute to the atherosclerotic lesion fibrous cap by PDGFRbeta and bioenergetic mechanisms. *Nat Metab.* 2021;3(2):166-81.
54. Salabei JK, and Hill BG. Autophagic regulation of smooth muscle cell biology. *Redox Biol.* 2015;4:97-103.
55. Kato F, Sakao S, Takeuchi T, Suzuki T, Nishimura R, Yasuda T, et al. Endothelial cell-related autophagic pathways in Sugen/hypoxia-exposed pulmonary arterial hypertensive rats. *Am J Physiol Lung Cell Mol Physiol.* 2017;313(5):L899-l915.
56. Kang R, Zeh HJ, Lotze MT, and Tang D. The Beclin 1 network regulates autophagy and apoptosis. *Cell Death Differ.* 2011;18(4):571-80.
57. Matsui Y, Takagi H, Qu X, Abdellatif M, Sakoda H, Asano T, et al. Distinct Roles of Autophagy in the Heart During Ischemia and Reperfusion. *Circulation Research.* 2007;100(6):914-22.
58. Jin Y, and Choi AM. Cross talk between autophagy and apoptosis in pulmonary hypertension. *Pulm Circ.* 2012;2(4):407-14.
59. Marquez RT, and Xu L. Bcl-2:Beclin 1 complex: multiple, mechanisms regulating autophagy/apoptosis toggle switch. *Am J Cancer Res.* 2012;2(2):214-21.
60. Takacs-Vellai K, Vellai T, Puoti A, Passannante M, Wicky C, Streit A, et al. Inactivation of the autophagy gene bec-1 triggers apoptotic cell death in C. elegans. *Curr Biol.* 2005;15(16):1513-7.
61. Jin Y, Ji Y, Song Y, Choe SS, Jeon YG, Na H, et al. Depletion of Adipocyte Becn1 Leads to Lipodystrophy and Metabolic Dysregulation. *Diabetes.* 2021;70(1):182-95.
62. Wendling O, Bornert JM, Chambon P, and Metzger D. Efficient temporally-controlled targeted mutagenesis in smooth muscle cells of the adult mouse. *Genesis.* 2009;47(1):14-8.

63. Sörensen I, Adams RH, and Gossler A. DLL1-mediated Notch activation regulates endothelial identity in mouse fetal arteries. *Blood.* 2009;113(22):5680-8.
64. Muzumdar MD, Tasic B, Miyamichi K, Li L, and Luo L. A global double-fluorescent Cre reporter mouse. *Genesis.* 2007;45(9):593-605.
65. Madisen L, Zwingman TA, Sunkin SM, Oh SW, Zariwala HA, Gu H, et al. A robust and high-throughput Cre reporting and characterization system for the whole mouse brain. *Nat Neurosci.* 2010;13(1):133-40.
66. Enge M, Bjarnegard M, Gerhardt H, Gustafsson E, Kalen M, Asker N, et al. Endothelium-specific platelet-derived growth factor-B ablation mimics diabetic retinopathy. *EMBO J.* 2002;21(16):4307-16.
67. Haase VH, Glickman JN, Socolovsky M, and Jaenisch R. Vascular tumors in livers with targeted inactivation of the von Hippel-Lindau tumor suppressor. *Proc Natl Acad Sci U S A.* 2001;98(4):1583-8.
68. Ryan HE, Poloni M, McNulty W, Elson D, Gassmann M, Arbeit JM, et al. Hypoxia-inducible factor-1alpha is a positive factor in solid tumor growth. *Cancer Res.* 2000;60(15):4010-5.
69. Gruber M, Hu CJ, Johnson RS, Brown EJ, Keith B, and Simon MC. Acute postnatal ablation of Hif-2alpha results in anemia. *Proc Natl Acad Sci U S A.* 2007;104(7):2301-6.